
The Prediction of STOVL Noise— Current Semi-Empirical Methods and Comparisions with Jet Noise Data

Paul T. Soderman, Ames Research Center, Moffett Field, California

April 1990



National Aeronautics and
Space Administration

Ames Research Center
Moffett Field, California 94035-1000

ABSTRACT

Current empirical models of several turbojet acoustic sources have been incorporated in a scheme for prediction of conventional or STOVL jet aircraft noise. The acoustic sources modeled were jet mixing noise, core noise, and broadband shock noise. The free-jet noise was then coupled with a new empirical equation for ground interaction noise generated by a vertically impinging jet. The modification of out-of-ground free-jet acoustic directivity pattern by a Harrier type nozzle installation was incorporated in the prediction of STOVL noise.

The jet/ground interaction noise prediction is the result of a flight test of the NASA Ames Harrier jet aircraft that was operated in vertical takeoff and landing. Acoustic data measured with an array of ground level microphones showed ground amplification of jet noise that peaked at a jet height equal to 18 nozzle diameters. At jet heights below 18 nozzle diameters, far-field ground level noise decreased. It is suggested that the noise decrease was caused by refraction of sound upward by the jet ground sheet. Near-field noise on the airframe was not measured, but published near-field data are examined.

Unlike numerous small-scale studies of jet impingement on a hard surface, in this study, no tones were found in the Harrier spectra. Implications for improved laboratory simulations of jet/ground interactions are discussed.

The acoustic prediction method described here gives fairly good agreement with measured far-field noise of the Harrier aircraft during hover in and out of ground effect.

NOMENCLATURE

A	nozzle area, m^2 , or polynomial coefficient
c	speed of sound, m/sec
d	effective diameter of one Harrier nozzle, m

d_h	nozzle hydraulic diameter, m
DI	directivity index defined as the difference between the noise at any angle and the noise at a reference angle.
f	frequency, Hz
h	altitude of exhaust nozzle centroid, m
L_p	sound pressure level, dB relative to 2×10^{-5} N/m ²
\dot{m}	jet mass flow rate, kg/sec
M	Mach number
P_3	combustor inlet pressure, Pa
r	source to observer distance, m
S	effective jet Strouhal number
T	absolute temperature, °K
v	velocity, m/sec
α	engine angle of attack, deg
ΔdB	change of noise level, dB
ψ	angle at nozzle between flight vector and r, deg, $\psi = \theta - \alpha$ for flyover
ρ	air density, kg/m ³
θ	angle at nozzle between jet axis (looking upstream) and r, deg
ω	density exponent (equation 3)

Figure 1 illustrates the angles and distances defined above.

Subscripts

a	ambient
c	convected or corrected
e	effective
g	effect of ground
n	nth microphone
ISA	international standard atmosphere (288 K and 101.3 kN/m ²)
j	fully expanded jet
o	aircraft or overall noise level
3	combustor inlet or third correction factor
4	combustor exit

INTRODUCTION

The prediction of STOVL (Short Takeoff and Vertical Landing) aircraft noise has become important to the airframe and propulsion system designer as the installed power of STOVL aircraft grows with mission requirements and the hazards from acoustically induced vibrations increase. In particular, there is considerable interest in a supersonic fighter aircraft that could take off on a short runway and land vertically. The ground environment of such a high thrust aircraft could be very hostile (1). The high noise generated during vertical landing in particular could: a) damage the aircraft or stores due to acoustically induced vibrations, b) induce destructive vibrations in the landing zone or ship, c) interfere with the pilot's communication and complicate his workload, d) cause ear damage or interfere with work of the ground crew, and e) expose large areas around the landing zone to relatively high noise levels. A key step in the control of this noise is the prediction of the acoustic field as a function of propulsion system so that designers can evaluate the acoustic tradeoffs of alternative systems.

Several airframe manufacturers recently participated in a NASA sponsored design study of US/UK STOVL fighter aircraft concepts. Each design team studied a different STOVL concept and evaluated it in terms of prescribed parameters such as propulsion performance, aerodynamics, weight, and so on. Part of that study required the estimation of the near-field and far-field acoustic environment of the aircraft.

Despite the variety of propulsion systems and the disparate groups involved, each design team relied heavily on the same report by Sutherland and Brown entitled "Prediction Methods for Near Field Noise Environment of VTOL Aircraft" (2) for the jet noise estimates. That work is an extensive compilation of small-scale studies, jet noise data, and empirical methodologies developed prior to 1972. The baseline jet noise model in that report is based on acoustic measurements of a J57-P21 jet engine by Hermes and Smith published in 1966 (3). Thus, each design team from the leading airframe manufacturers in this country relied, more or less, on the same small jet noise data base compiled 24 years ago. References 4 and 5 were also used by some of the design teams. This is not to suggest that the methods of Sutherland and Brown or the data of Hermes and Smith are incorrect. Indeed, those reports contain a wealth of information for the designer. However, in the last 24 years, substantial

progress has been made in the understanding of jet noise, and acoustic data for a wide range of configurations and operating conditions have been acquired that should improve the accuracy of jet noise prediction for various aircraft configurations.

The purpose of this paper is to illustrate a few of the current methods available for prediction of jet noise and to introduce a new empirical method for estimating ground amplification of jet noise during vertical landing or takeoff.

Vertical landing noise was the motivation for a flight test of a Harrier aircraft to be described. Although jet/ground interaction noise has been the subject of numerous laboratory studies of small jets (6), very limited large-scale jet data exist for this condition.

Furthermore, small-scale jet simulations often exhibit strong tones caused by a particular jet resonance. This resonance is not evident in Harrier noise data (7) and may be an artifact of small-scale jets because of the small Reynolds numbers. These scaling questions will be addressed further in STOVL jet noise studies being planned at Ames.

STOVL NOISE SOURCES

Following are the key aeroacoustic mechanisms responsible for STOVL jet noise. The radiation of these noise sources is modified by the forward speed of the aircraft and by the ground. The key equations used for jet noise prediction are included to illustrate the parameters and relationships involved, but the original references should be consulted for a complete explanation of the assumptions and data bases involved.

JET MIXING NOISE – The broadband noise generated by the energetic mixing of the jet stream within the core flow and in the shear layer between the jet and ambient air is the dominant noise source in subsonic jets. Jet mixing noise is also an important component of supersonic jet noise, especially for supersonic jets operating at the design nozzle pressure ratio where shock formation is weak.

Stone (8) derived empirical methods for the prediction of jet mixing noise that agree well with numerous data sets. These empirical equations contain parametric relationships that are consistent in most cases with analytical models of jet noise derived from first principles. Thus, Stone's equations are semi-empirical. It should be noted that the purely theoretical modeling of jet mixing noise is currently incomplete because of the lack of a dependable turbulence model.

For the prediction of single stream jet mixing noise, the required jet parameters are nozzle area, jet density, fully expanded jet velocity, aircraft flight speed, radiation distance and angle, and atmospheric sound speed and density (8). (Stone's method includes coaxial jet effects not included here.) The overall noise level is given by

$$L_{p_o} = 141 + 10 \log \left[\left(\frac{\rho_a}{\rho_{ISA}} \right)^2 \left(\frac{c_a}{c_{ISA}} \right)^4 \right] + 10 \log \left(\frac{A_j}{r^2} \right) + 10 \log \left(\frac{\rho_j}{\rho_a} \right)^\omega + 10 \log \left(\frac{v_e}{c_a} \right)^{7.5} - 15 \log \left[(1 + M_c \cos \theta)^2 + 0.04 M_c^2 \right] - 10 \log [1 - M_c \cos \psi] + 3 \log \left(\frac{2A_j}{\pi d_h^2} + \frac{1}{2} \right) \quad (1)$$

where

$$v_e = v_j \left[1 - \frac{v_o}{v_j} \cos \alpha \right]^{2/3} \quad (2)$$

is the effective jet velocity,

$$\omega = \frac{3 \left(\frac{v_e}{c_a} \right)^{3.5}}{0.6 + \left(\frac{v_e}{c_a} \right)^{3.5}} - 1 \quad (3)$$

is the density exponent, and

$$M_c = 0.62 (v_j - v_o \cos \alpha) / c_a \quad (4)$$

is the jet turbulence convection Mach number.

Spectra as a function of radiation angle can be estimated based on an effective Strouhal number (8), S .

$$S = \frac{f \sqrt{4A_j / \pi}}{v_e} \left(\frac{d_h}{\sqrt{4A_j / \pi}} \right)^{0.4} \left(\frac{T_j}{T_a} \right)^{0.4(1 + \cos \theta')} \times [1 - M_o \cos \psi] \times \left\{ \left[1 + 0.62 \left(\frac{v_j - v_o}{c_a} \right) \cos \theta \right]^2 + 0.01538 \left(\frac{v_j - v_o}{c_a} \right)^2 \right\}^{1/2} + \left\{ \left[1 + 0.62 \left(\frac{v_j}{c_a} \right) \cos \theta \right]^2 + 0.01538 \left(\frac{v_j}{c_a} \right)^2 \right\}^{1/2} \quad (5)$$

where the corrected directivity angle is:

$$\theta' = \theta (v_j / c_a)^{0.1} \quad (6)$$

The log of the Strouhal number is then used in Fig. 2 to obtain third-octave sound levels. The Appendix includes a subroutine which reads a polynomial fit to the curves and calculates third-octave noise levels.

Groen (9) found that the variation of sound level with jet velocity varies from V^3 to V^8 depending on the plume Mach number. Stone includes no such variation in his model.

Figures 3 and 4 show a comparison of jet mixing noise from equations 1 to 6 with data from a J85 turbojet operated at a static test site at NASA Ames (10). The data were measured on 12-m sideline. Considering the possible experimental errors caused by ground reflections, which were estimated and removed from the data, the agreement with prediction is good, both in terms of overall directivity (Fig. 3) and frequency spectra (Fig. 4).

CORE NOISE – It has been shown that the internally generated noise from engine combustion and turbulence, often called core noise, can radiate out the nozzle and contribute to jet mixing noise (11, 12). This is especially the case for subsonic jets in the forward direction during flight because jet mixing noise, comparatively weak in that direction, becomes weaker as the relative velocity between the jet and ambient air decreases with increasing airspeed (13), whereas core noise is less sensitive to the ambient airspeed. On the other hand, jet mixing noise increases with jet velocity to the eight power, approximately, whereas core noise increases with the fourth power of jet velocity. Thus, core noise should not be a factor with unsuppressed supersonic jets. In any case, the empirical methods for core noise are fairly easy to implement and should be

incorporated for STOVL noise predictions, particularly for the case of approach or departure from the landing zone.

The empirical methods of Motsinger and Emmerling (12) and Stone (11) for the estimation of turbojet engine core noise are straightforward. Their methods require turbine inlet and exit temperatures and pressure in the combustion zone, which are parameters available with engine data, but are seldom reported in acoustic papers. Hence, the accuracy of the prediction is difficult to verify from published acoustic data. Turbojet peak overall noise level 120° from the flight direction is given by

$$L_{p_o} = 56 - 20 \log \left[\dot{m} \left[(T_4 - T_3) \left(\frac{P_3}{P_a} \right) \left(\frac{T_a}{T_3} \right) \right]^2 \right] \quad (7)$$

The acoustic directivity described in Ref. 11 is used to obtain the noise at any other angle. A Doppler correction for the aircraft speed can be included. The core noise spectral shape can be estimated from the SAE jet mixing noise spectrum (14) modified so that the peak level is at 400 Hz. Motsinger and Emmerling (12) suggest that for core noise the difference between the peak third-octave sound level and the overall sound level is 6.8 dB.

Figure 5, which shows the difference between predicted mixing and core noise for a J85 turbojet, illustrates a trend from Eq. 7 that is consistent with data measured during a study of flight effects on J85 noise (13). That is, as mentioned above, the predicted jet mixing noise dominates the core noise at zero flight speed, but with forward speed, core noise becomes important relative to mixing noise toward the flight direction. In fact, the forward radiated noise can increase slightly in flight compared to zero flight speed despite the reduction of relative velocity between the jet and ambient air.

SHOCK NOISE – Shock noise is a complex phenomenon because of the many possible interactions between the jet flow and shock waves in the supersonic plume. Seiner (15) describes the physical mechanisms and acoustic characteristics of supersonic jets. The physics of supersonic jet noise is a current research topic at NASA Langley. For this paper, Stone's model of shock noise is used (8), which is based on the theory of Harper-Bourne and Fisher (16) and the experimental work of Seiner and Norum (17). The overall broadband shock noise at the observer angle ψ is given by

$$L_{p_o} = 162 + 10 \log \left[\left(\frac{p_a}{p_{ISA}} \right)^2 \left(\frac{c_a}{c_{ISA}} \right)^4 \right] + 10 \log \left(\frac{A_j}{r^2} \right) + 10 \log \left[\frac{(M_j^2 - 1)^2}{1 + (M_j^2 - 1)^2} \right] - 10 \log [1 - M_o \cos \psi] + F(\theta - \theta_M) \quad (8)$$

where the empirical constant

$$F = 0 \quad \text{for } \theta \leq \theta_M$$

$$F = -0.75 \quad \text{for } \theta > \theta_M$$

and

$$\theta_M = 180 - \sin^{-1} \frac{1}{M_j} \quad \text{is the Mach angle.}$$

The recommended third-octave spectrum shape is given in Ref. 8.

The shock noise model in equation 8 does not include the very strong tones which can occur from jet screech or eddy Mach wave radiation. These last two sources are difficult to predict without detailed information on the supersonic plume and shock structure (15). The frequencies of shock tones can be predicted in most cases.

Figure 6 illustrates the predicted components of mixing and shock noise compared to the measured spectrum from a model jet (18) operating under-expanded. These results suggest that, for this model jet, the mixing noise is responsible for the peak noise in the aft quadrant and shock noise dominates the forward quadrant.

JET/GROUND INTERACTION NOISE – When a vertical jet approaches the ground, the noise levels on the airframe and in the far field are amplified relative to free field levels by three effects: a) acoustic reflection by the ground, b) the alteration of the jet noise sources by aeroacoustic interactions with the ground, and c) the generation of new noise sources in the jet ground sheet. The jet ground sheet can also alter the propagation of noise to the far field by refraction of the sound waves.

The reflection of jet noise by the ground can be modeled mathematically by the summation of acoustic pressures from the real jet and an image jet located below the ground plane (2). The complete model includes a free-jet directivity factor and phase correlation between the direct and image sources.

However, Sutherland and Brown (2) found that agreement with data is best when phase correlation is ignored. Acoustic amplifications near the landing zone of up to 14 dB are predicted by this approach, but as the jet approaches the ground the prediction becomes inaccurate since jet directivity and source changes near the ground are difficult to predict.

Aeroacoustic interactions between the jet and ground have been the object of many small-scale studies. Most of these studies have focused on the intense tones from jets which have been excited by a feedback phenomenon involving instability waves in the mixing layer and upstream convecting acoustic waves originating in the impingement region. Ahuja and Spencer (6) found tones from impingement of a 13-mm-diameter jet that were 40 dB greater than the nonexcited jet spectrum. The maximum Reynolds number of their nozzle based on nozzle diameter was approximately 3×10^5 .

However, tones have not been identified in the limited large-scale data available, such as Harrier flight test data (7). In the case of the Harrier, it is not known if feedback tones were eliminated by high Reynolds number flow (12×10^6) or by multiple jet interactions. Preisser and Block (19) reported no tones in impingement studies of a single 64-mm diameter nozzle, presumably because of the sufficiently high Reynolds number flow (8×10^5).

Sutherland and Brown (2) suggest that the jet sheet on the ground can be a significant noise source, particularly in the near field of a subsonic jet. However, there is not sufficient information available on this source to develop a reliable acoustic prediction model.

Based on the uncertainties of modeling the jet/ground interaction noise sources described above, one must turn to empirical methods to estimate the total ground amplification. This is the primary reason we initiated the following study of a STOVL aircraft.

HARRIER FLIGHT TEST

A flight test of the NASA Ames AV-8C Harrier aircraft was conducted to develop an acoustic data base for vertical landing, vertical takeoff, and hover out of ground effect. The test was performed at the Naval Auxiliary Landing Field—Crows Landing, which is the same site used for a previous Harrier flight test reported by this author (7). The test described here was the more complete and accurate of the two. For example, measurement of noise during aircraft hover out of ground effect allowed us to establish the baseline jet radiation pattern. In the

previous study, SAE jet noise directivity curves had to be used (14), which were not directly applicable to the case of multiple jets issuing from the underside of an aircraft. In both studies, data were acquired with ground microphones in the acoustic far field of the jets.

HARRIER AV-8C – The Harrier aircraft, a swept-wing transonic fighter, utilizes four vectored nozzles for thrust and lift. It is capable of STOL or VTOL operation. Figures 7(a) and (b) are photographs of the NASA AV-8C aircraft. Figure 7(a) shows the nozzle deployment in vertical landing, and Fig. 7(b) shows the two fan inlets. Figure 8 is a schematic of the turbofan Pegasus engine used in the aircraft. The fan bypass air is exhausted from the two front nozzles and the turbine exhaust gas is exhausted from the two rear nozzles as shown. Typical temperatures and jet speeds for VTOL operation are noted. The rear jet Mach number is nominally 0.93.

The front and rear nozzle dimensions are given in Fig. 9. The nozzles are rectangular and cut parallel to the corner vanes shown in Fig. 9. That is, the exhaust area is not perpendicular to the duct axis. The effective diameter of an average nozzle, defined as the diameter of a duct with the same cross-sectional area as the average rectangular nozzles (measured perpendicular to the duct axis), is approximately 0.48 m. (This is the diameter used for h/d variation plots.) The hydraulic diameter of the exhaust nozzle, measured perpendicular to the nozzle exit is 0.52. (This hydraulic diameter was used in the noise prediction code.) With the aircraft on the ground, the center of the forward nozzle exhaust is 1.52 m above the ground, and the center of the aft nozzle exhaust is 1.22 m above the ground, for an average height of 1.35 m at the centroid of the nozzles.

Other sources of noise on the aircraft are the inlet fan and reaction-control jets. The primary acoustic array was oriented perpendicular to the side of the aircraft so as to avoid fan inlet noise. The reaction jet noise was not identified in the data.

TEST PROCEDURE – The aircraft was operated over a concrete runway with nine 12.7-mm-diameter condenser microphones positioned around the VTOL landing zone as shown in Fig. 10. The aircraft approached the landing site, hovered, and descended vertically at a rate around 0.8 m/sec. However, it is standard flight procedure to increase the throttle setting just before touchdown, followed by a sudden throttle cut before the wheels hit the ground. The throttle changes were visible in the

data, but were dominated by refraction effects at low aircraft altitude, as will be described.

After a cool-down, the aircraft took off vertically to the same altitude, hovered for several seconds, and descended uniformly again. The throttle setting is maximum during vertical takeoff, which causes the aircraft to accelerate to a speed around 5 m/sec before approaching hover. Although the throttle was not varied during takeoff, the rapid acceleration of the aircraft made it necessary to use a sequence of half-sec data samples for the plots of noise versus altitude rather than the one-sec averages used during landing. A number of landings and takeoffs were made.

The atmospheric conditions during the test were as follows:

Temperature	16° C (60° F)
Relative humidity	55 %
Barometric pressure	767 mm Hg (30.1 in Hg)
Wind	3 to 5 kts from the south

The microphones were laid on the ground and aimed at the landing target so as to obtain a uniform acoustic pressure reflection of 6 dB across the spectrum that was subtracted from the data. This procedure, which is recommended by the SAE for measuring jet noise (20), results in data free of valleys in the spectra caused by interference between the direct and ground reflected sound waves. Although the pressure doubling at the ground microphone is a ground interaction, it occurs no matter what altitude the source might be. Therefore, the 6 dB was removed from the raw data in order to highlight the ground interaction caused by aircraft proximity to the ground.

During all aircraft maneuvers, a laser radar tracking system was used. A laser beam was reflected from a reflector on the empennage that resulted in a continuous record of aircraft position to ± 0.3 m. The tracking data were correlated with time code that was also recorded on an acoustic data channel. Thus, the acoustic data could be accurately related to aircraft position at all times. The tracking system and time code were not available in the previous flight test (7), so aircraft position in that study was known only approximately. The results reported here are much more accurate.

DATA REDUCTION – Ideally, ground effects are best measured by keeping the aircraft and instrumentation fixed and moving the ground plane. In the flight test, however, the ground and microphones were fixed, and the noise source was moved. Thus, the distance from the noise source to the microphone and subsequent noise levels were constantly changing irrespective of the ground effect. Further-

more, jet noise is directional so that as the aircraft ascended or descended, the angle between the jet axis and the microphone changed, and the noise levels at the microphone changed irrespective of the ground effect. Both the distance and directivity effects had to be removed from the data so as to isolate the ground effect on the noise. Refraction of noise away from the ground microphone by the jet sheet near the ground could not be avoided.

The variable distance effect was removed by normalizing the data to the source-to-microphone distance with the aircraft at 30 m altitude using a free field decay rate (6 dB per double distance).

Noise variation from microphone to microphone caused by jet directivity was also removed from the data. The jet directivity pattern was measured with the microphone array on the ground and the aircraft hovering at nozzle centroid elevations of 12.2 m and 24.7 m. The aircraft was facing north. Using microphones 1 to 5 (Fig. 10), ten radiation angles were thereby obtained in the vertical plane perpendicular to the fuselage.

The complete corrections to the flight test data are summarized as follows:

$$L_{pc_n} = L_{p_n} + \Delta dB_1 + \Delta dB_2 + \Delta dB_3 \quad (9)$$

where

L_{pc_c} = corrected sound pressure level of the n th microphone with the aircraft at a normalized height of h/d , d is the effective diameter of one nozzle, 0.48 m, L_{p_n} = sound pressure level at the n th microphone as measured with the microphone flush with the ground, and

$$\Delta dB_1 = 20 \log \left(\frac{r_1}{r_2} \right) \quad \text{distance correction}$$

r_1 = distance from microphone to nozzle centroid

r_2 = distance from microphone to nozzle centroid at an arbitrary nozzle height of 30 m

$\Delta dB_2 = -6$ ground microphone reflection correction

$\Delta dB_3 = -DI(f, \theta)$ jet directivity index correction from equation 10 to be described.

Where appropriate, the overall sound levels without distance and angle corrections are plotted on the figures to represent the noise that would actually be heard at that aircraft and microphone position and operating condition.

FLIGHT TEST RESULTS – Figure 11 shows jet directivity patterns in the vertical plane 90° to the aircraft for selected third-octave frequencies. A third degree polynomial curve was fit through the data.

The data are plotted in terms of a directivity index, DI, defined as:

$$DI(f, \theta) = L_p(f, \theta) + 20 \log(r_n / 58) - L_p(f, 128^\circ) \quad (10)$$

where the second term extrapolates the data measured on the ground plane to a circle passing through microphone 4 with the exhaust nozzle centroid at an arbitrary altitude of 30 m. Equation 10 represents the difference in noise level at any angle θ from the noise measured 128° from the nozzle centroid, where 0° is upward. Thus, as the aircraft descended, the noise at a given microphone increased or decreased as the jet directivity lobe washed over the microphone. That noise change was removed from the data by subtracting the appropriate directivity index from the raw data.

As suspected, the directivity pattern of the Harrier jets issuing from the underside of the fuselage is different from that of a single, free jet. For comparison, isolated jet noise directivity from Ref. 14 is plotted on Fig. 11. The Harrier acoustic radiation pattern out of ground effect is closer to being omnidirectional than it is to the directivity of an isolated jet, presumably because of reflections from the fuselage and wing.

The radiation pattern in the horizontal plane at the ground during aircraft hover at 24.7-m nozzle altitude was acquired by the five microphones on the 30-m radius semicircle around the landing site. Zero degrees is the flight direction measured at the nozzle centroid. Figure 12 shows that peak noise occurred near 30° and 160° . The minimum at 90° may be due to jet shielding. In this figure, DI is simply the difference between the noise at any angle and the noise at 90° .

No tones were found in the data. Figures 13(a) and (b) show narrow-band acoustic spectra measured with the Harrier in and out of ground effect. The data measured during landing (Fig. 13(a)) have more scatter than the hover data (Fig. 13(b)) because of the fewer data samples acquired while the aircraft was moving. The lack of tones is a different result from many small-scale test results, which show intense tones from jet/ground interaction (6). As discussed above, this simulation problem is probably related to Reynold's numbers of model jets which are too small, or to multiple jet interactions on the Harrier not present in most small-scale tests.

EMPIRICAL MODEL OF GROUND-EFFECT NOISE

Figures 14(a) through (f) show 200, 1000, and 4000 Hz third-octave noise variations with normalized altitude, h/d , acquired 12.8 m to the side of the landing target (mic. 1) during a vertical takeoff and landing. Data with and without the corrections in Eq. 9 are plotted. The data show a maximum ground amplification of sound at around $h/d = 18$. Below that altitude the noise was weaker. This effect was clearly audible at the instrumentation van 65 m from the landing target.

The fact that the noise was less with the aircraft near the ground than at the hover position is probably due to refraction effects as the sound propagated to the microphones through the hot, turbulent ground jet sheet. That jet sheet would cause sound waves to refract upward. The refraction would have been strong for sound propagating parallel to the ground (low altitude jet) and weak for sound propagating more normal to the ground (high altitude jet). Thus, the sound heard at some distance above the ground microphones could actually be maximum with the jet near the ground.

The laboratory data of Preisser and Block (19) of a vertically impinging jet show a refraction effect indicated by low noise levels on the ground and high noise levels above the ground for a given jet height. The jet ground effect curves of Sutherland and Brown (2) have the same trend with increasing h/d as reported here, namely an initial increase in noise amplification followed by a decrease, possibly because of the jet refraction effect.

The ground amplification can be seen more clearly by plotting the difference in noise measured during hover (out of ground effect) and the noise at lower altitudes (in ground effect). Figures 15(a)-(d) show ground amplification based on a least square fit to landing and takeoff data from microphones 1 and 5, 12.8 m and 50 m from the landing target, respectively.

The change in far-field noise of a vertically exhausting jet by the ground can be represented by the following polynomial curves shown on Figs. 15(a)-(d).

$$\Delta dB_g = A_0 + A_1 \left(\frac{h}{d} \right) + A_2 \left(\frac{h}{d} \right)^2 + A_3 \left(\frac{h}{d} \right)^3 + A_4 \left(\frac{h}{d} \right)^4 + A_5 \left(\frac{h}{d} \right)^5 + A_6 \left(\frac{h}{d} \right)^6 \quad (11)$$

where the empirical coefficients A_i are listed in Table 1 for three third-octave frequencies during takeoff. Equation 11 is valid only for noise heard near the ground. At normalized jet heights below 18, the noise on the airframe is probably greater than that given by Eq. 11 for the reasons cited above.

Figure 16 compares ground amplification from Eq. 11 with small-scale, cold jet data reported by Sutherland and Brown (2). The small-scale data show much stronger ground effect than was measured with the Harrier. But it is not clear if the small-scale test is a poor simulation of full-scale jet engine aeroacoustics or if the refraction effects encountered in the Harrier test would account for the differences at small values of h/d .

It would appear that the Harrier ground amplification levels of 12 to 16 dB previously reported by this author (7) are 3 to 7 dB too high because of the lack of installed jet directivity patterns in that study. The use of free-jet directivity indices to correct the data resulted in incorrect levels of ground amplification.

Figures 17(a) and (b) compare the hover noise of the Harrier measured at microphone 4 with the complete set of predictions based on equations 1, 5, 7, and 11 (the jet was subsonic, so Eq. 8 was not needed). Results from hover at two altitudes are shown. The Harrier data were reduced by 6 dB to remove the pressure doubling at the microphone. Also the predicted noise from one aft nozzle was increased by 3 dB to account for the second nozzle. In addition, the predicted noise was modified by the difference between Harrier and free-jet directivity shown in Fig. 11. The predicted forward nozzle noise was at least 10 dB below the aft nozzle noise and is not shown.

The agreement between data and prediction in Fig. 17 is fairly good. It is possible that improvements could be made in the prediction if configuration effects such as nozzle shape and proximity to the airframe or multiple jet effects could be better accounted for in the method.

COMPUTER CODE

The Appendix is a listing of the computer code for jet noise prediction in and out of ground effect based on the above equations. The code was written in Microsoft QuickBASIC for the MAC II computer. QuickBASIC is a high level BASIC which can be compiled, and is similar in many ways to FORTRAN 77. A module is included for extrapolation of the predicted sideline levels to equal noise contours as a function of distance from the jet.

CONCLUDING REMARKS

Free-jet noise spectra are predicted using empirical equations from Stone and others. Turbojet mixing noise, core noise, and broadband shock noise models are described. The free-jet noise is then coupled with an empirical equation for ground interaction noise generated by a vertically impinging jet. Modifications to free-jet directivity by the Harrier nozzle installation were measured and can be incorporated in the prediction scheme.

The jet/ground interaction noise prediction is the result of a flight test of the Ames Harrier jet aircraft that was operated in vertical takeoff and landing. Acoustic data measured with an array of ground level microphones showed that ground-induced noise increased to around 9 dB relative to out-of-ground effect noise at a jet height of 18 nozzle diameters ($h/d = 18$). Below that height, the ground microphones recorded a decrease in noise relative to the peak noise condition. However, there is reason to believe that the noise attenuation below $h/d = 18$ was caused by refraction of the sound waves by the ground jet sheet which would have turned the sound upward away from the ground microphones. Although this effect would be beneficial to personnel and structures near the ground, it is likely that noise levels at some distance above the ground would continue to increase as the jet approached the impingement point.

No tones were found in the Harrier acoustic spectra. This suggests that small-scale simulations which show intense tones from jet impingement have jet flows with inadequate Reynolds numbers. However, it is also possible that multiple jet interactions inhibit jet/ground resonance tones.

The acoustic prediction method described here gives fairly good agreement with measured far-field noise of the Harrier aircraft during hover in and out of ground effect.

ACKNOWLEDGEMENT

The author wishes to thank the staff of the Ames Moffett Range Systems Branch for the excellent planning and execution of the flight test operations. The aircraft tracking system worked flawlessly. The experiment would have failed without the superb flying skills of Mike Stortz, Ames Flight Operations Branch, who was able to hold aircraft position and descent rate with exceptional accuracy.

REFERENCES

1. Knott, P. G.: The Ground Environment Created by High Specific Thrust Vertical Land Aircraft. Proceedings of International Powered Lift Conf. and Expos. P-203, SAE Paper 872309, pp. 75-85, Dec. 1987.
2. Sutherland, L. C. and Brown, D.: Prediction Method for Near Field Noise Environments of VTOL Aircraft. AFFDL-TR-71-180, AD 900405, May 1972.
3. Hermes, P. H. and Smith, D. L.: Measurement and Analysis of the J57-P21 Noise Field. AFFDL-TR-66-147, AD 403 713, Nov. 1966.
4. Ungar, E. E. et al.: A Review of Methods for Estimation of Aeroacoustic Loads on Flight Vehicle Surfaces. AFFDL-TR-76-91, Vol. II, Feb. 1977.
5. Ballantine, J. R., Passinos, B., and Plumblee, H. E. Jr.: Near Field Noise Analyses of Aircraft Propulsion Systems with Emphasis on Prediction Techniques for Jets. AFFDL-TR-67-43, Aug. 1967.
6. Ahuja, K. K. and Spencer, D. A.: Aeroacoustics of Advanced STOVL Aircraft Plumes. Proceedings of International Powered Lift Conf. and Expos., SAE, pp. 531-541, Dec. 1987.
7. Soderman, P. T. and Foster, J. D.: Noise of the Harrier in Vertical Landing and Takeoff. 1987 Ground Vortex Workshop, NASA CP-10008, pp. 167-190. Apr. 1987.
8. Stone, J. R.; Groesbeck, D. E.; and Zola, C. L.: Conventional Profile Coaxial Jet Noise Prediction. AIAA Journal, Vol. 21, No. 3, pp. 336-342, Mar. 1983.
9. Groen, D. S.: Acoustic Technologies for STOVL Aircraft. AIAA Paper 88-2238, 1988.
10. Hoglund, L. E.: Static Source Locations for Four Nozzles Mounted on a J-85 Engine. NASA CR-152401, Jan. 1979.
11. Stone, J. R.: Prediction of In-Flight Exhaust Noise for Turbojet and Turbofan Engines. Noise Control Engineering, Vol. 10, No. 1, pp. 39-46, Jan.-Feb. 1978.
12. Motsinger, R. E. and Emmerling, J. J.: Review of Theory and Methods for Combustion Noise Prediction. AIAA Paper 75-541, AIAA 2nd Aeroacoustics Conf., Mar. 1975.
13. Soderman, P. T.; Julienne, A.; and Atencio, A. Jr.: J85 Jet Engine Noise Measured in the ONERA S1 Wind Tunnel and Extrapolated to Far Field. NASA TP in publication.
14. SAE Committee A-21: Gas Turbine Jet Exhaust Noise Prediction, ARP 876B, Jun. 1981.
15. Seiner, J. M.: Advances in High Speed Jet Aeroacoustics. AIAA Paper 84-2275, AIAA-NASA 9th Aeroacoustics Conf., Oct. 1984.
16. Harper-Bourne, M. and Fisher, M. J.: The Noise from Shock Waves in Supersonic Jets. Noise Mechanisms, AGARD-CP-131, pp. 11-1 - 11-13, 1973.
17. Seiner, J. M. and Norum, T. D.: Experiments on Shock Associated Noise of Supersonic Jets. AIAA Paper 79-1526, July 1979.
18. Plumblee, H. E. Jr. et al.: The Generation and Radiation of Supersonic Jet Noise. Vol. II Studies of Jet Noise, Turbulence Structure and Laser Velocimetry. AFAPL-TR-76-65, Sept. 1976.
19. Preisser, J. S. and Block, P. J. W.: An Experimental Study of the Aeroacoustics of a Subsonic Jet Impinging Normal to a Large Rigid Surface. AIAA Paper 76-520, 3rd AIAA Aeroacoustics Conf., July 1976.
20. SAE Committee A-21: Practical Methods to Obtain Free-Field Sound Pressure Levels from Acoustical Measurements Over Ground Surfaces. SAE Aerospace Information Report 1672B, June 1983 (Appendix D).

APPENDIX—NOISE PREDICTION CODE

```

REM JET NOISE 4
REM Jet noise prediction based on the following papers:
REM 1) J. Stone: Convent. Profile Jet Noise Pred., AIAA Journal, V 21, No 3,
3/83
REM 2) J. Stone: Pred. of In-Flight Exhaust Noise for Turbojet and Turbofan
Engines,
REM Noise Control Eng., V 10, No 1, 1/78
REM 3) R. Molsinger AND J. Emmerling: Review of Theory and Methods for
REM Combustion Noise Prediction. AIAA Paper 75-541, 3/75
REM 4) SAE ARP 876B Gas Turbine Jet Exhaust Noise Prediction 6/81
REM 5) SAE ARP 866 Standard Values of Atmo. Absorption.... 8/64
REM This code predicts mixing, shock, and internal noise - overall & 1/3 oct
levels
REM Jet directivity for VTOL operation can be used
REM Ground amplification during VTOL operation can be computed
REM Written for MAC II computer using Microsoft QuickBASIC
REM Paul Soderman, NASA Ames Research Center, Moffett Field, CA 94035-
1000
REM Initial code 10/16/89, latest revision 3/15/90

```

```

CLEAR
OPTION BASE 1
DIM Lpomis(17),Theta(17),Thetar(17),R(17),Freq(19),Lptotal(17)
DIM Lpfnix(17,19),Splrefrac(11)
DIM
Lpshock(17),Lpshock(17,19),Sum(17),Lpshocksum(17),Lpomisum(17)
DIM
Lpocore(17),Lpfc(17,19),Lpcontour(17,9),Rcontour(17,9),Lpsum(17,19)
DIM Rstep(17),Contour(17),Lpmax(17),Oaspl(17),Delcore(17),Atten(19)
DIM Dist(61,17),Gndnoise(61,19),OAtotal1(61,17),OAtotal2(61,17),Sum2(17)
DIM LpfnixHD(17,19),LpfcHD(17,19),LpshockHD(17,19),Sum1(17)
DIM
Lpfree(11,17,19),Lpftotal(11,17,19),DelVTOL(17),Slope(11,2),Intercept(11,2)
DIM Acoef(4),Bcoef(4),Ccoef(11,9),Dcoef(2,9),Ecoef(7),Fcoef(7),Gcoef(7)

```

```

DEF FNlgt(X)=LOG(X)/LOG(10#) 'define log to base 10

```

```

*****
****
MainProgram:
GOSUB Device 'choose output device
GOSUB Constants 'set physical constants
GOSUB Getdata 'read data lines
GOSUB JetParameters 'user inputs on jet parameters
GOSUB ZeroArray 'zero out arrays
GOSUB MixingNoise 'compute overall jet mixing noise
GOSUB MixSpectra 'compute third oct jet mixing noise
IF Q2$="A" OR Q2$="a" THEN GOTO 2 'no internal noise
GOSUB CoreNoise 'compute internal noise if real engine
2:IF Shock$="N" THEN GOTO 5 'no shocks
GOSUB ShockNoise 'compute overall shock noise
GOSUB ShockSpectra 'compute third oct shock noise
5:IF Q4$="N" OR Q4$="n" THEN GOTO 6 'use free jet directivity
GOSUB VTOL 'directivity of Harrier type VTOL jets
6:IF Q5$="N" OR Q5$="n" THEN GOTO 7 'no ground effect
GOSUB GroundEffect 'ground effect from Soderman
7:IF Q6$="N" OR Q6$="n" THEN GOTO 8 'compute noise on sideline only
GOSUB NoiseContours 'compute equal noise contours
8:GOSUB Table 'print results
END

```

```

*****
****
Device:

```

```

Act=0 'choose output device
Sw=SYSTEM(5) 'dialog parameter
Sh=SYSTEM(6) 'get screen width (640 - MACII)
WINDOW 2,"",(2*Sw,.2*Sh)-(.7*Sw,.7*Sh),2 'get screen height (480 - MACII)
PRINT "Choose output device"
Ww=WINDOW(2) 'window width
Wh=WINDOW(3) 'window height
BUTTON 1,1,"Output to screen",(.2*Ww,.3*Wh)-(.8*Ww,.4*Wh),1
'buttons in window
BUTTON 2,1,"Output to laser writer",(.2*Ww,.5*Wh)-(.8*Ww,.6*Wh),1
EDIT FIELD 1,"Return key defaults to laser writer",(.2*Ww,.7*Wh)-
(.9*Ww,.8*Wh),1
TEDEACTIVATE WINDOW(6) 'turn off blinking insertion point
ON DIALOG GOSUB HandleAct: DIALOG ON 'turn on dialog
WHILE Act=0 'idle first time through
WEND
GOTO ExitSub
HandleAct: 'respond to button or return key
Act=DIALOG(0) 'gives type of response
ON Act GOSUB ButtonChoice,Default,Rien,Rien,Rien,Default
RETURN
ButtonChoice:
Buttonpushed=DIALOG(1) 'remember which button
pushed, 1 or 2
RETURN
Rien: 'return
RETURN
Default: 'return key hit
Buttonpushed=2 'make equivalent to button 2, laser writer
RETURN
ExitSub:
DIALOG OFF 'turn off dialog
TEACTIVATE WINDOW(6) 'restore blinking insertion
point
WINDOW CLOSE 2 'close window
RETURN

```

```

*****
****
Constants:
Ca=341 'ambient sound speed, m/s
Pi=3.141593 'pi
Patm=1.0133*10^5 'atmos. pressure (sea level, std day),
N/m^2
Tatm=288 'atmos. temperature (sea level, std day), °K
Rho=1.225 'atmos. density (sea level, std day),
kg/m^3
Gasconst=287.07 'gas constant (for deg K)
Conv=Pi/180 'conversion of degrees to radians

PRINT "This program computes jet mixing noise of an isentropic round jet"
PRINT "plus shock and internal noise if applicable"
PRINT " "
RETURN

```

```

*****
****
Getdata:

PRINT "Stand by .....":PRINT ""
DATA 40,45,50,60,70,80,90,100,110,120,130,135,140,145,150,155,160

```

DATA
125,160,200,250,315,400,500,630,800,1000,1250,1600,2000,2500,3150
DATA 4000,5000,6300,8000

DATA 1.3833,9.208,-1.3121,3.6711

DATA 1.4234,-3.2606,-3.2349,1.0938

DATA -11.0675,-1199,-9.1572,2.2075,-.4772,-.41195,.08067,.020897,-
.006838
DATA -10.4187,-2.956,-13.1197,4.2334,2.8791,-.9321,-.4322,.0505,.0201
DATA -11.6827,-10.8374,-9.2813,8.3173,-.3826,-1.717,.2968,.09026,-.01867
DATA -12.7804,-14.8857,-6.5027,8.9098,-2.8374,-1.6376,.8172,.082,-.04574
DATA -14.6415,-17.7705,-7.2519,9.9263,-2.4613,-1.8954,.7275,.09659,-
.04082
DATA -19.7458,-19.0679,-5.5739,8.5806,-2.7099,-1.4602,.6879,.07107,-
.03703
DATA -25.8693,-22.4106,-2.8185,8.0779,-3.8488,-1.2806,.8886,.06089,-
.04702
DATA -30.8276,-24.4745,-3147,7.8722,-5.6792,-1.1883,1.2988,.05478,-.069
DATA -33.2332,-25.3239,.8815,7.5701,-6.1164,-1.1384,1.4252,.0521,-
.07625
DATA -35.4555,-25.865,-3554,7.1344,-5.5769,-1.0676,1.3056,.04847,-
.06984
DATA -62.4274,-24.6076,-.5718,-.9541,.571,-.8605,-.4659,-.05531,.03126

DATA 24.722,4,-12,-5.6
DATA 27.556,9.202,-12,-8.4
DATA 30.333,14.2,-13,-12
DATA 33.167,19.4,-16,-12.9
DATA 33.278,19.8,-18,-15.2
DATA 33.611,21,-19,-20.2
DATA 34.722,25,-21,-26.3
DATA 30,18,-22,-31
DATA 25,10,-23,-33.3
DATA 20,2,-24,-35.5
DATA 14.556,-7.6,-25,-62.5

DATA 0,1,.5,1.1,4,-3.2,-5.8,-7.7,-9,-10.6,0

DATA 0,-.7768,-9.0222,5.31684,-2.6109,-2.9839,2.6279,.6055,-.5677
DATA 0,-5.6935,-22.6928,4.2535,27.7981,.5425,-20.4298,-.2422,4.4278

DATA 9,8,5,8,7,5,9,4,7,3,5,2,4,1,2,0,0,1,1,8,2,8,3,9,5

DATA 3,3,3,3,3,3,4,4,3,0,-2.5,-3,-5,-6.5,-8,-8.5,-9

DATA .1,2,.4,.5,7,1,1,1,1,1,2,1,5,2,2,5,3,4,5,8,9,12,21.5

DATA -1599,-28598,5320,-313.8,8.552,-.11289,.0005878

DATA -130587,39793,-3023,122,-2.782,.032996,-.00015985

DATA -68531,21545,-931.5,-5.035,1.215,-.027562,.00019022

FOR Ang=1 TO 17 'jet directivity angles, 0° is flight direction
 READ Theta(Ang) 'degrees (read data)
 Thetar(Ang)=Theta(Ang)*Conv 'radians
NEXT Ang

FOR I = 1 TO 19
 READ Freq(I) 'third-oct band center frequencies data
NEXT I

FOR I=1 TO 4 'curve fit (P&W Aeronautical Handbook)
 READ Acoef(I) 'polynomial coeff for specific heat ratio air
NEXT I '400° to 1600° R

FOR I=1 TO 4 'curve fit
 READ Bcoef(I) 'polynomial coeff for specific heat ratio air/fuel
NEXT I '800° to 2000° R

FOR I=1 TO 11
 FOR J=1 TO 9
 READ Ccoef(I,J) 'spectra correction parameters - Table 1, ref. 1
 NEXT J 'polynomial coeff for curve fit; -1.8<log
S<1.8
NEXT I

FOR I=1 TO 11
 READ Slope(I,1) 'table 1 linear curve fit; log S<-1.8
 READ Intercept(I,1)
 READ Slope(I,2) 'table 1 linear curve fit; log S>1.8
 READ Intercept(I,2)
NEXT I

FOR K=1 TO 11
 READ Splrefrac(K) 'refraction correction to OASPL - Table 1
NEXT K

FOR I=1 TO 2
 FOR J=1 TO 9
 READ Dcoef(I,J) 'core noise
 NEXT J 'polynomial coeff for spectra curve fit - ARP 867B
NEXT I

FOR Ang=1 TO 17
 READ Delcore(Ang) 'core noise directivity factor - ref. 1
NEXT Ang

FOR Ang=1 TO 17
 READ DelVTOL(Ang) 'VTOL noise directivity factor
(Soderman)
NEXT Ang

FOR I=1 TO 19
 READ Aten(I) 'extrapolation to noise contours
NEXT I 'air absorption parameters
 'dB/1000 ft at each 1/3 oct band

FOR J=1 TO 7
 READ Ecoef(J) 'polynomial coeff for ground amplification
 Ecoef(J)=Ecoef(J)*.0001 'low frequencies (Soderman)
NEXT J

FOR J=1 TO 7
 READ Fcoef(J) 'polynomial coeff for ground amplification
 Fcoef(J)=Fcoef(J)*.0001 'mid frequencies (Soderman)
NEXT J

FOR J=1 TO 7
 READ Gcoef(J) 'polynomial coeff for ground amplification
 Gcoef(J)=Gcoef(J)*.0001 'high frequencies (Soderman)
NEXT J

RETURN

```

*****
****
JetParameters:
    'user inputs of jet parameters
LINE INPUT "Input description of test case",Proj$
INPUT "Is this a round, single stream nozzle ?",Noz$
IF Noz$="Y" OR Noz$="y" THEN
    INPUT "Input nozzle diameter",Dia
    Area=Pi*Dia^2/4          'area of exhaust nozzle, m^2
ELSE
    INPUT "Input nozzle hydraulic diameter, m ",Dia
    INPUT "Input nozzle perimeter,m ",Perim
    Area=Dia*Perim/4
END IF
INPUT "Input jet total temperature, deg K ",Ttot
INPUT "Input aircraft speed, m/s ",Va
INPUT "Input sideline (horizontal) distance from jet centerline to receiver, m
,Sideline
10: LINE INPUT "Is this an air jet or combustion jet (a or c) ?",Q2$
    Shock$="Y"              'assume supersonic jet until calculated
otherwise
    Trank=Ttot*1.8          'jet temperature in degrees Rankine

SELECT CASE Q2$
CASE "A","a"              'specific heat ratio for air jet-curve fit
    Gama=Acoef(1)+Acoef(2)*10^-5*Trank+Acoef(3)*10^-7*Trank^2
    Gama=Gama+Acoef(4)*10^-11*Trank^3
CASE "C","c"              'specific heat ratio for jet combustion
    Gama=Bcoef(1)+Bcoef(2)*10^-5*Trank+Bcoef(3)*10^-8*Trank^2
    Gama=Gama+Bcoef(4)*10^-11*Trank^3
CASE ELSE
    PRINT "Wrong answer, try again"
    GOTO 10
END SELECT

Gama=INT((Gama+.005)*100)/100    'round off
PRINT "  Pr is jet pressure ratio.  Vj is jet exhaust velocity."
20: LINE INPUT "Do you want to input Pr or Vj (p or v) ? ",Q3$

SELECT CASE Q3$
CASE "P","p"
    INPUT "Input jet pressure ratio ",Pr
    Tj=Ttot*(Pr^((1-Gama)/Gama))    'static temperature in jet
    Mach=SQR((Pr^((Gama-1)/Gama)-1)/((Gama-1)/2))    'jet Mach
number
    Cj=SQR(Gama*Gasconst*Tj)        'sound speed in jet, m/s
    Vj=Mach*Cj                      'jet speed, m/s
    Vj=INT((Vj+.05)*10)/10          'round off
CASE "V","v"
    INPUT "Input jet velocity, m/s ",Vj
    Cp=Gasconst*Gama/(Gama-1)        'specific heat
    Tj=(Cp*Ttot-Vj^2/2)/Cp            'static temperature in jet
    Cj=SQR(Gama*Gasconst*Tj)        'sound speed in jet, m/s
    Mach=Vj/Cj                      'jet Mach number
    Pr=(1+((Gama-1)*Mach^2)/2)/(Gama/(Gama-1))    'jet pressure ratio
    Pr=INT((Pr+.005)*100)/100        'round off
CASE ELSE
    PRINT "Wrong answer, try again"
    GOTO 20
END SELECT

Tj=INT(Tj+.5)
LINE INPUT "Do you want to use Harrier type VTOL jet directivity ?",Q4$
LINE INPUT "Do you want to compute ground effect in VTOL operation ?",Q5$
LINE INPUT "Do you want to compute equal noise contours ? ",Q6$

```

```

IF Q6$="Y" OR Q6$="y" THEN
    INPUT "What is maximum distance to contours, m ?",Maxdist
END IF
IF Mach<1 THEN
    Shock$="N"
    PRINT " "
    PRINT "Jet Mach number is less than 1, no shock noise will be computed"
ELSE
    PRINT "Jet Mach number is greater than 1, shock noise will be computed"
END IF

PRINT " "
Density=Patm/(Gasconst*Tj)          'compute isentropic flow conditions
'jet density, assume Pjet=Patm,
kg/m^3
Rhoratio=Density/Rho                'ratio of jet density to ambient density
Mdot=Density*Area*Vj                'jet mass flow rate, kg/s
Thrust=Mdot*Vj                      'jet thrust, N
Mo=Va/Ca                            'aircraft Mach number
RETURN

*****
****
ZeroArray:
    'set arrays to zero

FOR Ang=1 TO 17
    FOR I=1 TO 19
        Lpfmix(Ang,I)=0
        Lpfc0re(Ang,I)=0
        Lpfshock(Ang,I)=0
        Lpfsum(Ang,I)=0
    NEXT I
    Lpocore(Ang)=0
    Sum(Ang)=0
NEXT Ang
RETURN

*****
****
MixingNoise:
    'Appendix equations in ref. 1
    'standard day, zero angle of attack
    FOR Ang = 1 TO 17
        R(Ang)=Sideline/SIN(Thetar(Ang))    'distance to observer on sideline
        Ve=Vj*(1-Va/Vj)^.667                'effective jet velocity
        W=3*(Ve/Ca)^3.5/((.6+(Ve/Ca)^3.5)-1    'density exponent
        Mc=.62*(Vj-Va)/Ca                    'convection Mach number
        Aa=10*FNlgt(Rhoratio^W)
        Bb=10*FNlgt((Ve/Ca)^7.5)
        Cc=15*FNlgt((1+Mc*COS(Thetar(Ang)))^2+.04*Mc^2)
        Dd=10*FNlgt(1-Mo*COS(Thetar(Ang)))
        Ee=141+10*FNlgt(Area/(R(Ang))^2)
        Ff=3*FNlgt(2*Area/(Pi*Dia^2)+.5)
        Lpomix(Ang)=Aa+Bb-Cc-Dd+Ee+Ff        'overall mixing noise
        R(Ang)=INT((R(Ang)+.05)*10)/10        'round off
    NEXT Ang
    PRINT "OASPL mixing noise computed":PRINT ""
RETURN

*****
****
MixSpectra:
    'Table 1 in ref. 1
    'compute spectral effects-appendix ref. 1
    'factors in effective Strouhal equation
    C1=(4*Area/Pi)^.5

```

```

C2=C1/Ve
C3=(Dia/C1)^.4          'diameter is jet hydraulic diameter

FOR Ang=1 TO 17          'angle loop
  Thetap=Thetar(Ang)*(Vj/Ca)^.1
  Thetapo=INT((Thetap/Conv+.05)*10)/10
  C4=(Ttot/Tatm)^(.4*(1+COS(Thetap)))
  C5=1-Mo*COS(Thetar(Ang))
  C6=(1+.62*((Vj-Va)/Ca)*COS(Thetar(Ang)))^2
  C7=.01538*((Vj-Va)/Ca)^2
  C8=(1+.62*(Vj/Ca)*COS(Thetar(Ang)))^2
  C9=.01538*(Vj/Ca)^2
  FOR I=1 TO 19          'frequency loop
    St=Freq(I)*C2*C3*C4*C5*((C6+C7)^.5)/((C8+C9)^.5)
    Sto=FNlgt(St)

    IF Thetapo<=110 THEN JJ=1
    IF Thetapo>110 AND Thetapo<=120 THEN JJ=2
    IF Thetapo>120 AND Thetapo<=130 THEN JJ=3
    IF Thetapo>130 AND Thetapo<=140 THEN JJ=4
    IF Thetapo>140 AND Thetapo<=150 THEN JJ=5
    IF Thetapo>150 AND Thetapo<=160 THEN JJ=6
    IF Thetapo>160 AND Thetapo<=170 THEN JJ=7
    IF Thetapo>170 AND Thetapo<=180 THEN JJ=8
    IF Thetapo>180 AND Thetapo<=190 THEN JJ=9
    IF Thetapo>190 AND Thetapo<=200 THEN JJ=10
    IF Thetapo>200 AND Thetapo<=250 THEN JJ=11

    IF Sto<-1.8 THEN      'match Thetapo with angle in Table 1, ref. 1
      Spectrap2=Slope(JJ,1)*Sto+Intercept(JJ,1)
      Spectrap1=Spectrap2
    ELSEIF Sto>1.8 THEN
      Spectrap2=Slope(JJ,2)*Sto+Intercept(JJ,2)
      Spectrap1=Spectrap2
    ELSE
      Spectrap2=Ccoef(JJ,1)+Ccoef(JJ,2)*Sto+Ccoef(JJ,3)*Sto^2
      Spectrap2=Spectrap2+Ccoef(JJ,4)*Sto^3+Ccoef(JJ,5)*Sto^4
      Spectrap2=Spectrap2+Ccoef(JJ,6)*Sto^5+Ccoef(JJ,7)*Sto^6
      Spectrap2=Spectrap2+Ccoef(JJ,8)*Sto^7+Ccoef(JJ,9)*Sto^8
      Spectrap1=Spectrap2
    IF JJ>1 THEN
      Spectrap1=Ccoef(JJ-1,1)+Ccoef(JJ-1,2)*Sto+Ccoef(JJ-1,3)*Sto^2
      Spectrap1=Spectrap1+Ccoef(JJ-1,4)*Sto^3+Ccoef(JJ-1,5)*Sto^4
      Spectrap1=Spectrap1+Ccoef(JJ-1,6)*Sto^5+Ccoef(JJ-1,7)*Sto^6
      Spectrap1=Spectrap1+Ccoef(JJ-1,8)*Sto^7+Ccoef(JJ-1,9)*Sto^8
    END IF
  END IF
  Thetapo2=JJ*10+100      'extrapolate between directivity angles
  Spectrap=Spectrap2-((Thetapo2-Thetapo)/10)*(Spectrap2-Spectrap1)
  IF JJ=11 THEN
    Thetapo2=250
    Spectrap=Spectrap2-((Thetapo2-Thetapo)/50)*(Spectrap2-Spectrap1)
  END IF

  Lpfmix(Ang,I)=Lpomix(Ang)+Spectrap 'mixing noise third oct levels, dB
  Lpfmix(Ang,I)=INT((Lpfmix(Ang,I)+.05)*10)/10 'round off
  Sum(Ang)=Sum(Ang)+10^(Lpfmix(Ang,I)/10) 'sum of press squares
NEXT I
PRINT "Lpfmix computed for ";Theta(Ang); " deg"
NEXT Ang
PRINT ""

FOR Ang = 1 TO 17
  Lpomixsum(Ang)=10*FNlgt(Sum(Ang)) 'integrate to get OASPL
  Lpomixsum(Ang)=INT((Lpomixsum(Ang)+.05)*10)/10 'round off

  Lptotal(Ang)=Lpomixsum(Ang)          'total sound if no shock or core
  noise
NEXT Ang
RETURN

*****
****
CoreNoise:
          'internal engine noise, overall and 1/3 oct
P3=Pr*Patm          '*****rough estimate of combustor inlet pressure
T3=1.5*Tatm          '*****rough estimate of combustor inlet temperature

Trise=(Ttot-T3)          'combustor temperature rise, °K
Lpref=56-20*FNlgt(R(10))          'find OASPL at theta = 120° (ref. 2, 3)
Lpref=Lpref+10*FNlgt(Mdot*(Trise*(P3/Patm)*(Tatm/T3))^2)

FOR Ang=1 TO 17
  Lpocore(Ang)=Lpref-Delcore(Ang)-20*FNlgt(R(Ang)/R(10)) 'OASPL
directivity ref. 2
  Lpocore(Ang)=Lpocore(Ang)-40*FNlgt(1-(Mo*COS(Thetar(Ang)))) 'flight
effect
  Lpocore(Ang)=INT((Lpocore(Ang)+.05)*10)/10 'round off
NEXT Ang

'third-oct spectral shapes are taken from SAE ARP 876B
'but spectra are centered on 400 Hz, which is different than ARP 876B
FOR Ang=1 TO 17          'angle loop
  FOR I=1 TO 19          'frequency loop
    Ff=FNlgt(Freq(I)/400) 'spectrum freq parameter set relative to 400 Hz
    D90=Dcoef(1,1)+Dcoef(1,2)*Ff+Dcoef(1,3)*Ff^2+Dcoef(1,4)*Ff^3
    D90=D90+Dcoef(1,5)*Ff^4+Dcoef(1,6)*Ff^5+Dcoef(1,7)*Ff^6
    D90=D90+Dcoef(1,8)*Ff^7+Dcoef(1,9)*Ff^8
    D160=Dcoef(2,1)+Dcoef(2,2)*Ff+Dcoef(2,3)*Ff^2+Dcoef(2,4)*Ff^3
    D160=D160+Dcoef(2,5)*Ff^4+Dcoef(2,6)*Ff^5+Dcoef(2,7)*Ff^6
    D160=D160+Dcoef(2,8)*Ff^7+Dcoef(2,9)*Ff^8
    Delspl=D90+(D160-D90)*SIN(Ang*Pi/(17*2)) 'spectrum shape factor
    Lpfcore(Ang,I)=Lpocore(Ang)+Delspl-6.8 'third oct core noise (ref. 3)
    Lpfcore(Ang,I)=INT((Lpfcore(Ang,I)+.05)*10)/10 'round off
    F1=Lpfmix(Ang,I)/10
    F2=Lpfcore(Ang,I)/10
    Lpfsum(Ang,I)=10*FNlgt(10^F1+10^F2)
    Lpfsum(Ang,I)=INT((Lpfsum(Ang,I)+.05)*10)/10 'sum of mix+internal
  I/3 OB
NEXT I
  N1=Lpomixsum(Ang)/10
  N2=Lpocore(Ang)/10
  Lptotal(Ang)=10*FNlgt(10^N1+10^N2)
  Lptotal(Ang)=INT((Lptotal(Ang)+.05)*10)/10 'sum of mix + internal
OASPL
  PRINT "Lpfcore computed for ";Theta(Ang); " deg"
NEXT Ang
PRINT ""
RETURN

*****
****
ShockNoise:
          'equations 4a-4b, ref. 1
FOR Ang=1 TO 17
  Thetam=180-ATN(1/SQR(Mach^2-1))/Conv 'Mach angle, deg
  IF Theta(Ang)>Thetam THEN
    Factor=-.75          'empirical constant
  ELSE

```

```

Factor=0
END IF
A1=162+10*FNlgt(Area/(R(Ang))^2)
A2=10*FNlgt((Mach^2-1)^2/(1+(Mach^2-1)^2))
A3=-10*FNlgt(1-Mo*COS(Thetar(Ang)))
A4=Factor*(Theta(Ang)-Thetam)
Lposhock(Ang)=A1+A2+A3+A4 'overall noise level from shocks, dB
Lposhock(Ang)=INT((Lposhock(Ang)+.05)*10)/10 'round off
NEXT Ang
RETURN

*****
****
ShockSpectra:
'equation 5, ref. 1

b1=Dia/(.7*Vj)

FOR Ang=1 TO 17
Sum(Ang)=0 'clear spectral summation
parameter
NEXT Ang

FOR Ang=1 TO 17
B2=SQR(Mach^2-1)*(1-Mo*COS(Thetar(Ang)))
B3=SQR((1+.7*(Vj/Ca)*COS(Thetar(Ang)))^2+.0196*(Vj/Ca)^2)
FOR I=1 TO 19
Stshock=Freq(I)*b1*B2*B3
Stshock=FNlgt(Stshock)

IF Stshock<-.12 THEN 'fig. 3 linear curve fit, ref. 1
B4=50.85*Stshock-3.5
ELSEIF Stshock>0 THEN
B4=-10.56*Stshock-7
ELSE
B4=25*Stshock-7
END IF

Lpfshock(Ang,I)=Lposhock(Ang)+B4 'third oct shock noise levels, dB
Lpfshock(Ang,I)=INT((Lpfshock(Ang,I)+.05)*10)/10
F1=Lpfmix(Ang,I)/10
F2=Lpfcocore(Ang,I)/10
F3=Lpfshock(Ang,I)/10
Lpfsum(Ang,I)=10*FNlgt(10^F1+10^F2+10^F3) 'sum
mix+internal+shock 1/3 OB
IF Q2$="A" OR Q2$="a" THEN 'no core noise
Lpfsum(Ang,I)=10*FNlgt(10^F1+10^F3) 'sum mix+shock 1/3 OB
END IF
Lpfsum(Ang,I)=INT((Lpfsum(Ang,I)+.05)*10)/10
Sum(Ang)=Sum(Ang)+10^(Lpfshock(Ang,I)/10)
NEXT I
Lposhocksum(Ang)=10*FNlgt(Sum(Ang)) 'alternatively, integrate to get
OASPL
Lposhocksum(Ang)=INT((Lposhocksum(Ang)+.05)*10)/10
N1=Lposhocksum(Ang)/10
N2=Lpomixsum(Ang)/10
N3=Lpocore(Ang)/10
Lptotal(Ang)=10*FNlgt(10^N1+10^N2+10^N3)
Lptotal(Ang)=INT((Lptotal(Ang)+.05)*10)/10 'sum of mix + shock +
internal OASPL
PRINT "Lpfshock computed for ";Theta(Ang);" deg"
NEXT Ang
RETURN

```

```

*****
****
VTOL: 'compute VTOL jet directivity based on
'Harrier data recorded by Soderman
DeIVTOL is Harrier DI-Freejet DI
'where DI is the directivity index

FOR Ang=1 TO 17
Lpomixsum(Ang)=Lpomixsum(Ang)+DeIVTOL(Ang)
IF Shock$="Y" THEN
Lposhocksum(Ang)=Lposhocksum(Ang)+DeIVTOL(Ang)
IF Q2$="c" THEN Lpocore(Ang)=Lpocore(Ang)+DeIVTOL(Ang)
Lptotal(Ang)=Lptotal(Ang)+DeIVTOL(Ang)
FOR I=1 TO 19
Lpfmix(Ang,I)=Lpfmix(Ang,I)+DeIVTOL(Ang)
IF Shock$="Y" THEN Lpfshock(Ang,I)=Lpfshock(Ang,I)+DeIVTOL(Ang)
IF Q2$="c" THEN Lpfcocore(Ang,I)=Lpfcocore(Ang,I)+DeIVTOL(Ang)
Lpfsum(Ang,I)=Lpfsum(Ang,I)+DeIVTOL(Ang)
NEXT I
NEXT Ang
RETURN

*****
****
GroundEffect:

Count=0 'compute jet noise in VTOL ground effect
FOR HD=1 TO 31 STEP 3 'loop on jet height to dia ratio
Count=Count+1

FOR Ang=1 TO 17
Sum1(Ang)=0 'clear summation parameters
Sum2(Ang)=0
NEXT Ang

FOR Ang=1 TO 17
Dist(HD,Ang)=SQR(R(Ang)^2+(HD*Dia)^2) 'distance to receiver, m
FOR I=1 TO 19 'use poly curve fit at each freq
IF Freq(I)<600 THEN 'based on Harrier ground effect data
DI=Ecoef(1)+Ecoef(2)*HD+Ecoef(3)*HD^2+Ecoef(4)*HD^3
DI=DI+Ecoef(5)*HD^4+Ecoef(6)*HD^5+Ecoef(7)*HD^6
ELSEIF Freq(I)>590 AND Freq(I)<2500 THEN
DI=Fcoef(1)+Fcoef(2)*HD+Fcoef(3)*HD^2+Fcoef(4)*HD^3
DI=DI+Fcoef(5)*HD^4+Fcoef(6)*HD^5+Fcoef(7)*HD^6
ELSEIF Freq(I)>2490 THEN
DI=Gcoef(1)+Gcoef(2)*HD+Gcoef(3)*HD^2+Gcoef(4)*HD^3
DI=DI+Gcoef(5)*HD^4+Gcoef(6)*HD^5+Gcoef(7)*HD^6
END IF
Gndnoise(HD,I)=DI 'ground amplification of jet noise
LpfmixHD(Ang,I)=Lpfmix(Ang,I)-20*FNlgt(Dist(HD,Ang)/R(Ang))
N1=LpfmixHD(Ang,I)/10
Lpfree(Count,Ang,I)=LpfmixHD(Ang,I) 'jet noise corrected
IF Q2$="C" OR Q2$="c" THEN
LpfcocoreHD(Ang,I)=Lpfcocore(Ang,I)-20*FNlgt(Dist(HD,Ang)/R(Ang))
N2=LpfcocoreHD(Ang,I)/10
Lpfree(Count,Ang,I)=10*FNlgt(10^N1+10^N2) 'jet noise corrected
END IF
IF Shock$="Y" THEN
LpfshockHD(Ang,I)=Lpfshock(Ang,I)-
20*FNlgt(Dist(HD,Ang)/R(Ang))
N3=LpfshockHD(Ang,I)/10
Lpfree(Count,Ang,I)=10*FNlgt(10^N1+10^N2+10^N3) 'jet noise
corrected
END IF

```



```

N4=Lpfree(Count,Ang,I)/10
Lpftotal(Count,Ang,I)=Lpfree(Count,Ang,I)+Gndnoise(HD,I) 'corrected
for ground
N5=Lpftotal(Count,Ang,I)/10
Sum1(Ang)=Sum1(Ang)+10^N4
Sum2(Ang)=Sum2(Ang)+10^N5
Lpfree(Count,Ang,I)=INT((Lpfree(Count,Ang,I)+.05)*10)/10 'round off
Lpftotal(Count,Ang,I)=INT((Lpftotal(Count,Ang,I)+.05)*10)/10 'round
off
NEXT I
OAtotal1(HD,Ang)=10*FNlgt(Sum1(Ang)) 'overall free jet noise
OAtotal1(HD,Ang)=INT((OAtotal1(HD,Ang)+.05)*10)/10 'round off
OAtotal2(HD,Ang)=10*FNlgt(Sum2(Ang)) 'overall free+gnd jet noise
OAtotal2(HD,Ang)=INT((OAtotal2(HD,Ang)+.05)*10)/10 'round off
PRINT "Ground effect computed for ";Theta(Ang);" deg at H/D =";HD
Dist(HD,Ang)=INT((Dist(HD,Ang)+.05)*10)/10 'round off
NEXT Ang
NEXT HD
RETURN

*****
****
NoiseContours: 'compute equal noise contours for free jet
'no ground effect included
'ARP 866 air absorp, std day, 70% RH
PRINT "Compute noise contours":PRINT""
Rmin=Maxdist-1
FOR Ang=1 TO 17
Rstep(Ang)=R(Ang) 'extrapolation distance
Contour(Ang)=0
FOR K=1 TO 9
Rcontour(Ang,K)=0 'clear contour parameters
Lpcontour(Ang,K)=0
NEXT K
NEXT Ang
WHILE Rmin<Maxdist
FOR Ang = 1 TO 17
Sum(Ang)=0
IF Rstep(Ang)<Rmin THEN Rmin=Rstep(Ang)
FOR I=1 TO 19
N1=10^(Lpfmix(Ang,I)/10) 'mixing noise 1/3 oct
N2=10^(Lpfcocore(Ang,I)/10) 'internal noise 1/3 oct
N3=10^(Lpfshock(Ang,I)/10) 'shock noise 1/3 oct
Total=10*FNlgt(N1+N2+N3) '1/3 oct noise at ref distance
Total=Total-20*FNlgt(Rstep(Ang)/R(Ang)) 'total noise corrected for
spread
Total=Total-Atten(I)*(Rstep(Ang)-R(Ang))/(.3048*1000) 'correct for air
Sum(Ang)=Sum(Ang)+10^(Total/10) 'sum of pressure square in
each band
NEXT I
Oaspl(Ang)=10*FNlgt(Sum(Ang)) 'corrected overall sound level
Oaspl(Ang)=INT(Oaspl(Ang)+.5) 'round up, e.g. 134.5 goes to 135
IF Oaspl(Ang)/10=Oaspl(Ang)/10 THEN 'true if Oaspl divisible by 10
Contour(Ang)=Contour(Ang)+1 'number of contours at this angle
K=Contour(Ang)
IF K>9 THEN GOTO 40 'dimension limit
Lpcontour(Ang,K)=Oaspl(Ang) 'sound level on contour
Rcontour(Ang,K)=Rstep(Ang) 'distance to contour
IF K=1 THEN GOTO 40 'only 1 Lp per contour (following line)

```

```

IF Lpcontour(Ang,K)=Lpcontour(Ang,K-1) THEN Rcontour(Ang,K)=0
40 :
END IF
Rstep(Ang)=Rstep(Ang)+10 'move out 10 meters
NEXT Ang
PRINT "Rmin =";Rmin;"m"
Rmin=Rmin+10
WEND
RETURN

*****
****
Table:
Times=20 'print results
Plain=0 'define font
'define text face
SELECT CASE Buttonpushed
CASE 1
OPEN"SCRN:" FOR OUTPUT AS #1 'output to screen
CASE ELSE
OPEN"LPT1:" FOR OUTPUT AS #1 'output to laser writer
END SELECT
WINDOW OUTPUT #1
WIDTH #1,255 'set maximum line width for no word wrap
CALL TEXTFONT(Times) 'set text attributes
CALL TEXTSIZE(12)
CALL TEXTFACE(Plain)

----- print header -----
PRINT#1,TAB(80);DATES
PRINT#1,TAB(30);"JET NOISE 4",TAB(80);TIMES
PRINT#1,TAB(80);"P. Soderman"
PRINT#1,TAB(20);Proj$
PRINT#1,""
PRINT#1,TAB(20);"Flight speed =";Va;" m/s"
PRINT#1,TAB(20);"Jet speed =";Vj;" m/s"
PRINT#1,""
PRINT#1,TAB(20);"Jet total temperature =";Ttot;" deg K"
PRINT#1,TAB(20);"Jet static temperature =";Tj;" deg K"
PRINT#1,TAB(20);"Jet pressure ratio =";Pr
IF Q4$="N" OR Q4$="n" THEN PRINT#1,TAB(20);"Free jet directivity model"
IF Q4$="Y" OR Q4$="y" THEN PRINT#1,TAB(20);"VTOL jet directivity
model"
PRINT#1,""
PRINT#1,TAB(20);"Jet nozzle hydraulic dia =";Dia;" m"
PRINT#1,TAB(20);"Ratio of jet density to ambient";
PRINT#1,USING " ### ";Rhoratio
PRINT#1,TAB(20);"Specific heat ratio";Gama
PRINT#1,""
PRINT#1,TAB(20);"Jet Mach number =";
PRINT#1,USING " ###";Mach
PRINT#1,TAB(20);"Mass flow rate =";
PRINT#1,USING " ####.## ";Mdot;
PRINT#1,TAB(42);"kg/s"
PRINT#1,TAB(20);"Thrust =";
PRINT#1,USING " #####.##";Thrust;
PRINT#1,TAB(38);"N"
PRINT#1,"":PRINT #1,TAB(20);"Overall free field noise levels on
sideline":PRINT #1,""

----- print overall mixing noise levels only -----

```

```

IF (Shock$="N") AND (Q2$="A" OR Q2$="a") THEN 'mixing noise only
PRINT#1,TAB(21);"Integrated";TAB(30);"Distance to"
PRINT#1,TAB(10);" Theta Lpomix Sideline, m"
PRINT " "

```

```

FOR Ang=1 TO 17
PRINT#1,TAB(10);
PRINT#1,Theta(Ang);TAB(22);Lpomixsum(Ang);TAB(32);R(Ang)
NEXT Ang
CALL TEXTFONT(Times) 'set text attributes in case of new page
CALL TEXTSIZE(12)
CALL TEXTFACE(Plain)

```

----- print overall mixing + shock noise -----

```

ELSEIF (Shock$="Y") AND (Q2$="A" OR Q2$="a") THEN 'mix + shock
noise
PRINT#1,TAB(21);"Integrated Integrated";TAB(50);"Distance to"
PRINT#1,TAB(10);" Theta Lpomix Lposhock Lptotal
Sideline, m"
PRINT " "

```

```

FOR Ang=1 TO 17
PRINT#1,TAB(10);

```

```

PRINT#1,Theta(Ang);TAB(20);Lpomixsum(Ang);TAB(30);Lposhocksum(Ang);
TAB(40);
PRINT#1,Lptotal(Ang);TAB(50);R(Ang)
NEXT Ang
CALL TEXTFONT(Times) 'set text attributes in case of new page
CALL TEXTSIZE(12)
CALL TEXTFACE(Plain)

```

----- print overall mixing + shock + internal noise -----

```

ELSE 'mix + shock + internal noise
PRINT#1,TAB(20);"Integrated Integrated";TAB(60);"Distance to"
PRINT#1,TAB(10);" Theta Lpomix Lposhock Lpcore
Lptotal Sideline, m"
PRINT " "

```

```

FOR Ang=1 TO 17
PRINT#1,TAB(10);

```

```

PRINT#1,Theta(Ang);TAB(20);Lpomixsum(Ang);TAB(30);Lposhocksum(Ang);
TAB(40);Lpcore(Ang);
PRINT#1,TAB(50);Lptotal(Ang);TAB(60);R(Ang)
NEXT Ang
CALL TEXTFONT(Times) 'set text attributes in case of new page
CALL TEXTSIZE(12)
CALL TEXTFACE(Plain)

```

```

END IF
PRINT " "

```

----- print overall noise with ground effect -----

```

IF Q5$="Y" OR Q5$="y" THEN
PRINT#1,CHR$(12) 'page advance
CALL TEXTFONT(Times) 'set text attributes in case of new page
CALL TEXTSIZE(12)
CALL TEXTFACE(Plain)
PRINT#1,"":PRINT#1,TAB(20);"Overall noise levels during VTOL on
ground":PRINT #1,""
PRINT#1,TAB(20);"Integrated Integrated" 'free jet + ground effect noise

```

```

PRINT#1,TAB(10);" Theta Lpo_free Delta Gnd Lpo_gnd
Sideline, m R, m"

```

```

FOR HD=1 TO 31 STEP 3
PRINT#1,""
PRINT#1,TAB(10);"Jet height to diameter ratio =";HD:PRINT#1,""
FOR Ang=1 TO 17
Gndamp=OAtotal2(HD,Ang)-OAtotal1(HD,Ang)
Gndamp=INT((Gndamp+.05)*10)/10

```

```

PRINT#1,TAB(10);Theta(Ang);TAB(20);OAtotal1(HD,Ang);TAB(30);Gndamp;

```

```

PRINT#1,TAB(40);OAtotal2(HD,Ang);TAB(50);R(Ang);TAB(60);Dist(HD,Ang)
NEXT Ang
CALL TEXTFONT(Times) 'set text attributes in case of new page
CALL TEXTSIZE(12)
CALL TEXTFACE(Plain)
NEXT HD
PRINT#1,CHR$(12) 'page advance

```

----- print third oct noise in and out of ground effect -----

```

PRINT#1,"":PRINT#1,TAB(20);"Third octave spectra during VTOL on
ground":PRINT#1,""
PRINT#1,TAB(60);"Distance to"
PRINT#1,TAB(10);" Theta Freq, Hz Lpfree(f) Lpgnd(f) Delta
Gnd(f) Sideline, m"
PRINT#1," "

```

```

Count=0
FOR HD=1 TO 31 STEP 3
Count=Count+1
PRINT#1,""
PRINT#1,TAB(10);"Jet height to diameter ratio =";HD:PRINT#1,""
FOR Ang=7 TO 17 STEP 6
FOR I=2 TO 19 STEP 2
Gndamp=Lpftotal(Count,Ang,I)-Lpfree(Count,Ang,I)
Gndamp=INT((Gndamp+.05)*10)/10

```

```

PRINT#1,TAB(10);Theta(Ang);TAB(20);Freq(I);TAB(30);Lpfree(Count,Ang,I);

```

```

PRINT#1,TAB(40);Lpftotal(Count,Ang,I);TAB(50);Gndamp;TAB(60);R(Ang)
CALL TEXTFONT(Times) 'set text attributes in case of new page
CALL TEXTSIZE(12)
CALL TEXTFACE(Plain)
NEXT I
PRINT#1,""
NEXT Ang
NEXT HD

```

```

GOTO QuitTable 'skip free field third-oct printout
END IF
PRINT#1," "

```

----- print third oct free field mixing noise -----

```

PRINT#1,"":PRINT#1,TAB(20);"Third octave spectra on sideline":PRINT #1,""
PRINT#1,"":PRINT#1,TAB(20);"Third octave free field spectra on
sideline":PRINT #1,""
IF (Shock$="N") AND (Q2$="A" OR Q2$="a") THEN 'mixing noise only
PRINT#1,TAB(40);"Distance to"
PRINT#1,TAB(10);" Theta Freq, Hz Lpmix(f) Sideline, m"
PRINT#1," "

```

```

FOR Ang=1 TO 1 'remove for entire directivity pattern

```

```

FOR Ang=1 TO 17
  FOR I=1 TO 19
    PRINT#1,TAB(10);

PRINT#1,Theta(Ang);TAB(20);Freq(I);TAB(30);Lpfmix(Ang,I);TAB(40);R(Ang
)
  CALL TEXTFONT(Times)      'set text attributes in case of
new page
  CALL TEXTSIZE(12)
  CALL TEXTFACE(Plain)
  NEXT I
  PRINT#1,""
NEXT Ang

'----- print third oct free field mixing + shock noise -----

ELSEIF (Shock$="Y") AND (Q2$="A" OR Q2$="a") THEN      'mix +
shock noise
  PRINT#1,TAB(60);"Distance to"
  PRINT#1,TAB(10);" Theta      Freq, Hz      Lpmix(f)      Lpshock(f)
Lptotal(f)      Sideline, m"
  PRINT#1,""

  FOR Ang=1 TO 1          'remove for entire directivity pattern
  FOR Ang=1 TO 17
    FOR I=1 TO 19
      PRINT#1,TAB(10);

PRINT#1,Theta(Ang);TAB(20);Freq(I);TAB(30);Lpfmix(Ang,I);TAB(40);Lpfsho
ck(Ang,I);
  PRINT#1,TAB(50);Lpfsum(Ang,I);TAB(60);R(Ang)
  CALL TEXTFONT(Times)      'set text attributes in case of new page
  CALL TEXTSIZE(12)
  CALL TEXTFACE(Plain)
  NEXT I
  PRINT#1,""
NEXT Ang

'----- print third oct free field mixing + shock + internal noise -----

ELSE      'mix + shock + internal noise
  PRINT#1,TAB(70);"Distance to"
  PRINT#1,TAB(10);" Theta      Freq, Hz      Lpmix(f)      Lpshock(f)
Lpcore(f)      Lptotal(f)      Sideline, m"
  PRINT#1,""

  FOR Ang=1 TO 1          'remove for entire directivity
pattern
  FOR Ang=1 TO 17
    FOR I=1 TO 19

PRINT#1,TAB(10);Theta(Ang);TAB(20);Freq(I);TAB(30);Lpfmix(Ang,I);
  PRINT#1,TAB(40);Lpshock(Ang,I);TAB(50);Lpcore(Ang,I);TAB(60);
  PRINT#1,Lpfsum(Ang,I);TAB(70);R(Ang)
  CALL TEXTFONT(Times)      'set text attributes in case of new page
  CALL TEXTSIZE(12)
  CALL TEXTFACE(Plain)
  NEXT I
  PRINT#1,""
NEXT Ang

END IF
PRINT#1,""

'----- print equal free field noise contours OASPL -----

IF Q6$="Y" OR Q6$="y" THEN      'print equal noise contours for OASPL
  PRINT#1," "
  PRINT#1,TAB(10);"Distance in meters to contours of overall noise"
  PRINT#1,TAB(10);"Distance decay and atmospheric attenuation included"
  PRINT#1," "
  PRINT#1,TAB(10);" Theta      Lpcontour      Rcontour, m"
  PRINT#1," "

  FOR Ang=1 TO 17
    FOR K=1 TO 7
      IF Rcontour(Ang,K)=0 THEN GOTO 80
      PRINT#1,TAB(10);

PRINT#1,Theta(Ang);TAB(22);Lpcontour(Ang,K);TAB(37);Rcontour(Ang,K)
80 : NEXT K
  CALL TEXTFONT(Times)      'set text attributes in case of new page
  CALL TEXTSIZE(12)
  CALL TEXTFACE(Plain)
  NEXT Ang

END IF
QuitTable:
IF Buttonpushed=1 THEN INPUT"Hit RETURN to continue",Dum      'output to
screen
PRINT#1, CHR$(12)      'page advance
CLOSE#1      'nothing prints on paper until device is closed
CLS      'clear screen
RETURN

```

Table 1 – Polynomial coefficients for Eq 11

Frequency, Hz	i	A _i
200	0	-0.1599
	1	-2.8598
	2	0.5320
	3	-0.03138
	4	0.0008552
	5	-1.1289×10^{-5}
	6	5.8780×10^{-8}
1000	0	-13.0587
	1	3.9793
	2	-0.3023
	3	0.0122
	4	-0.0002782
	5	3.2996×10^{-6}
	6	-1.5985×10^{-8}
4000	0	-6.8531
	1	2.1545
	2	-0.09315
	3	-0.0005035
	4	0.0001215
	5	-2.7562×10^{-6}
	6	1.9022×10^{-8}

Coefficients from 6° polynomial curve fit to third-octave band data recorded at microphone 1 during a vertical takeoff.

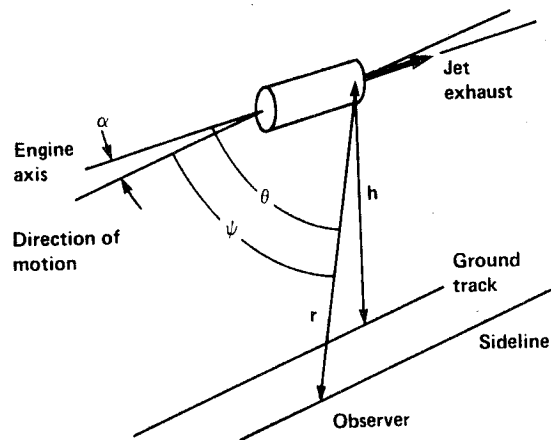


Figure 1 – Geometric distances and angles relative to jet nozzle.

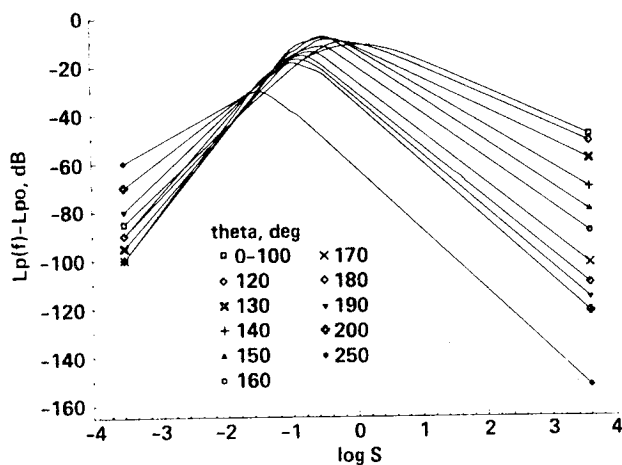


Figure 2 – Recommended third-octave spectra for jet mixing noise from Ref. 8. S is the effective Strouhal number from Eq. 5. θ is the corrected directivity angle from Eq. 6.

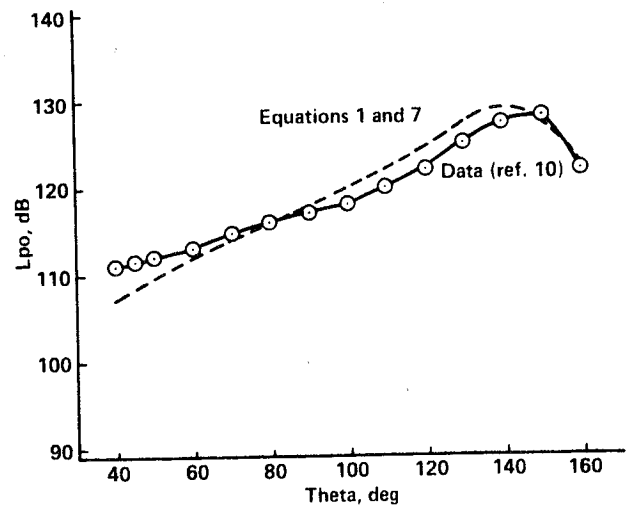


Figure 3 – Predicted and measured overall noise of a J85 turbojet along a 12-m sideline; $d = 0.44$ m, $v_j = 514$ m/s, $v_o = 0$, $M_j = 0.99$, $T_j = 819^\circ$ K, pressure ratio = 1.83.

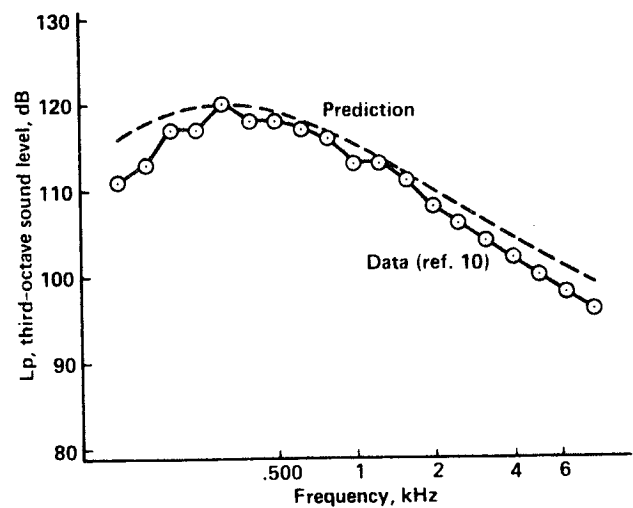


Figure 4 – Predicted and measured third-octave noise of a J85 turbojet for the conditions of Fig. 3; $\theta = 140^\circ$.

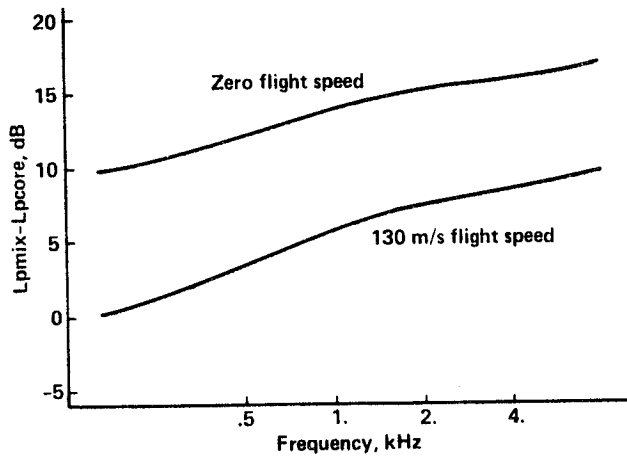


Figure 5 – The predicted difference between J85 turbojet mixing and core noise at flight speeds of 0 and 130 m/sec, $\theta = 45^\circ$ (Eq. 7).

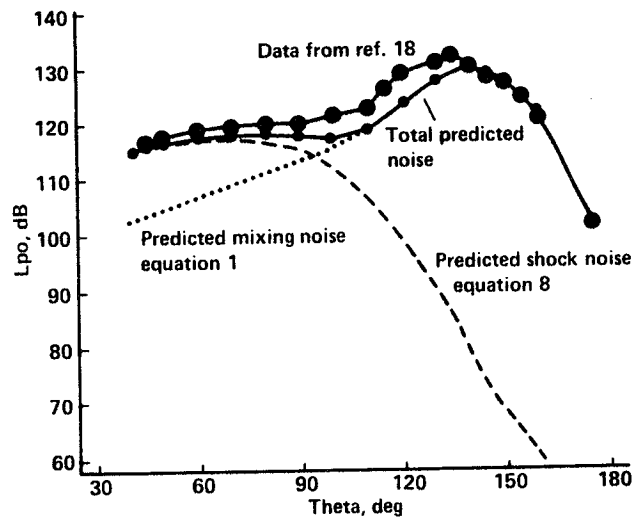
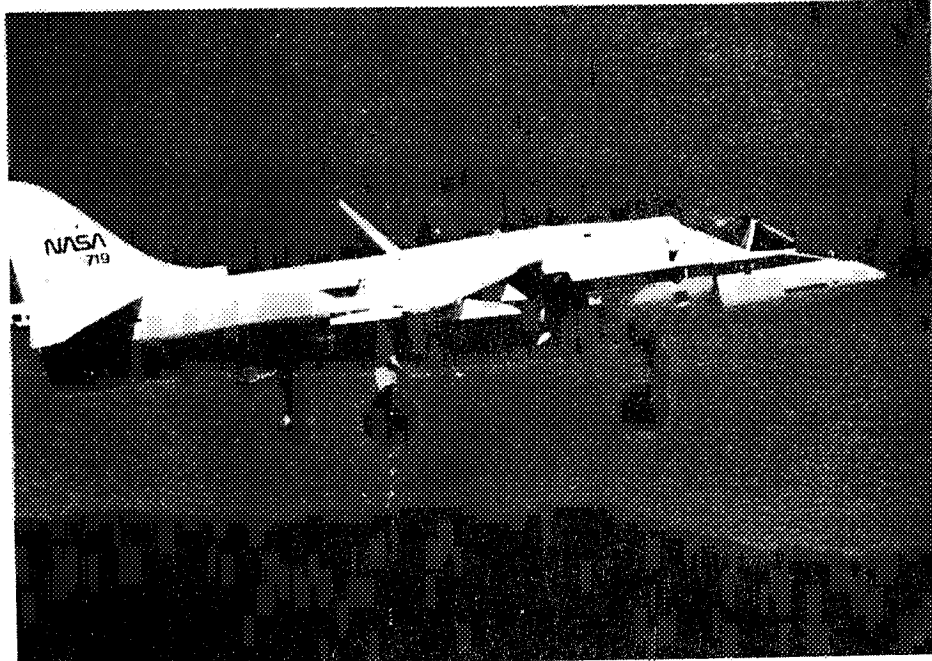
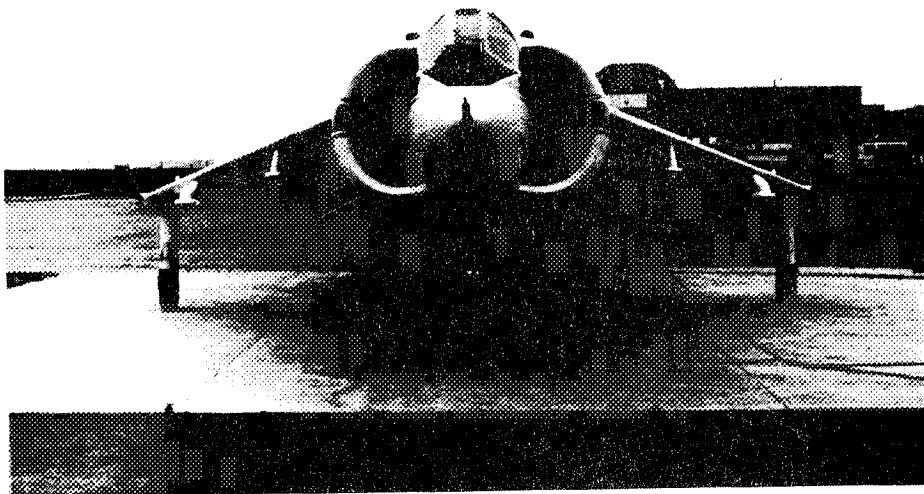


Figure 6 – Predicted and measured jet mixing and broadband shock noise of a 51-mm-diam hot jet on a 3.7-m sideline. $M_j = 1.38$, $T_o = 634^\circ \text{ K}$, underexpanded.



(a) Side view during hover



(b) Front view on ground

Figure 7 – Ames AV8C Harrier aircraft.

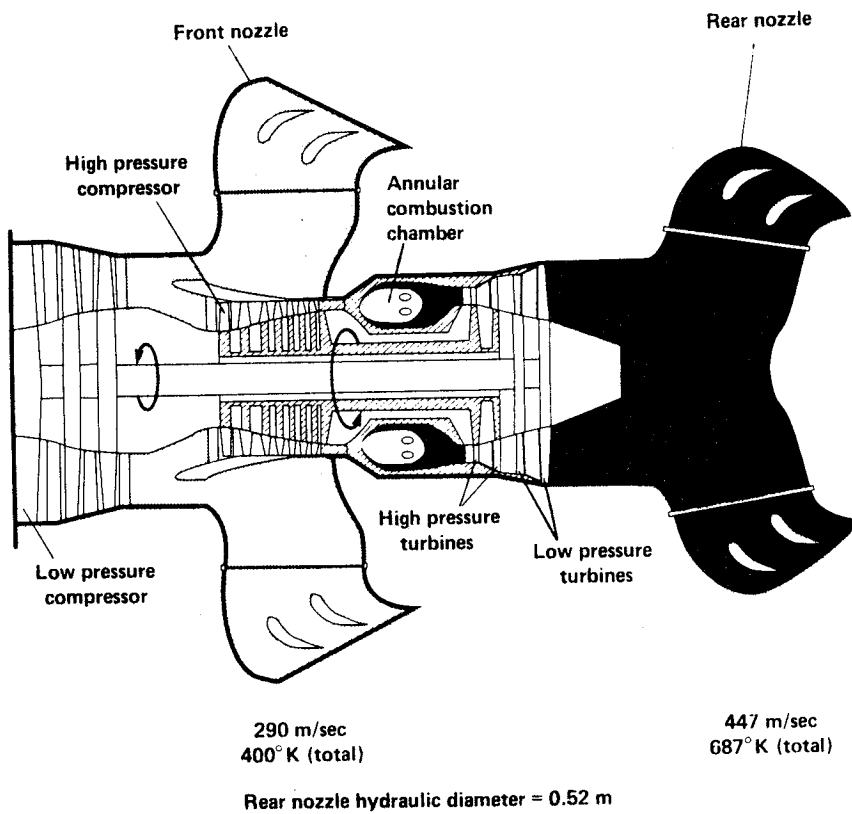


Figure 8 – Pegasus engine and exhaust ducting. Velocities and temperatures are for nominal VTOL operation.

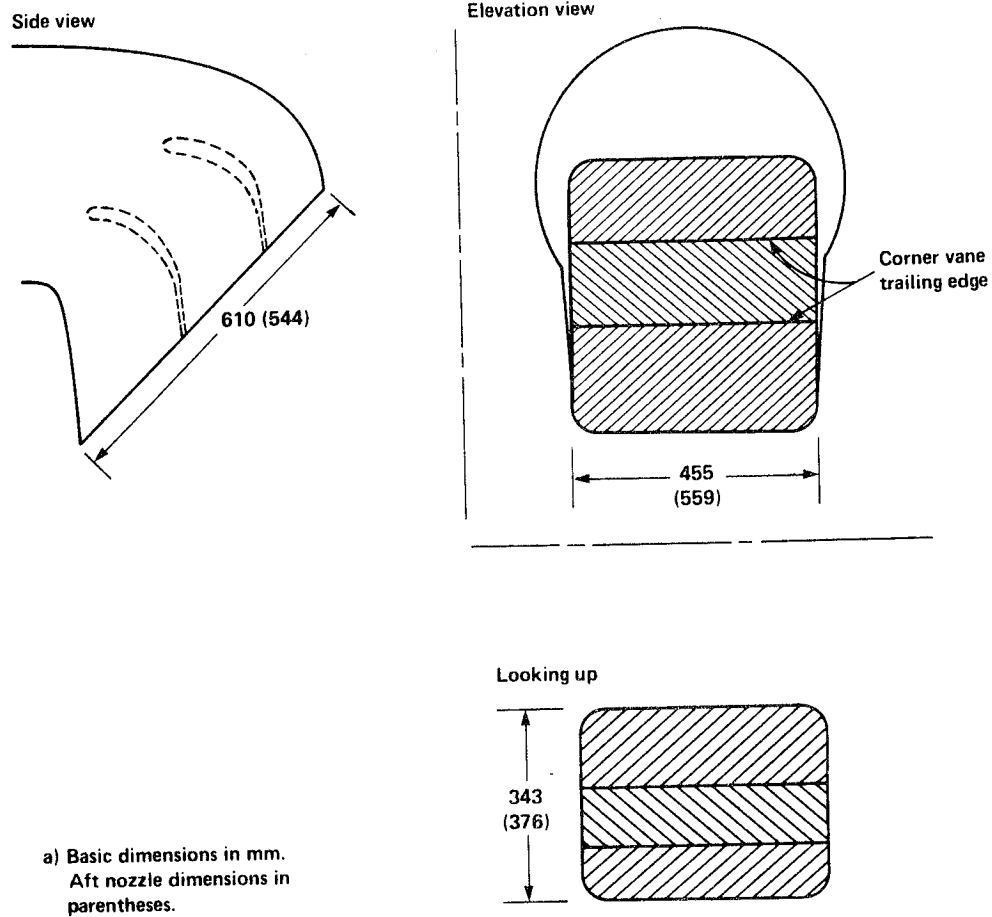


Figure 9 – Exhaust nozzle geometry and dimensions.

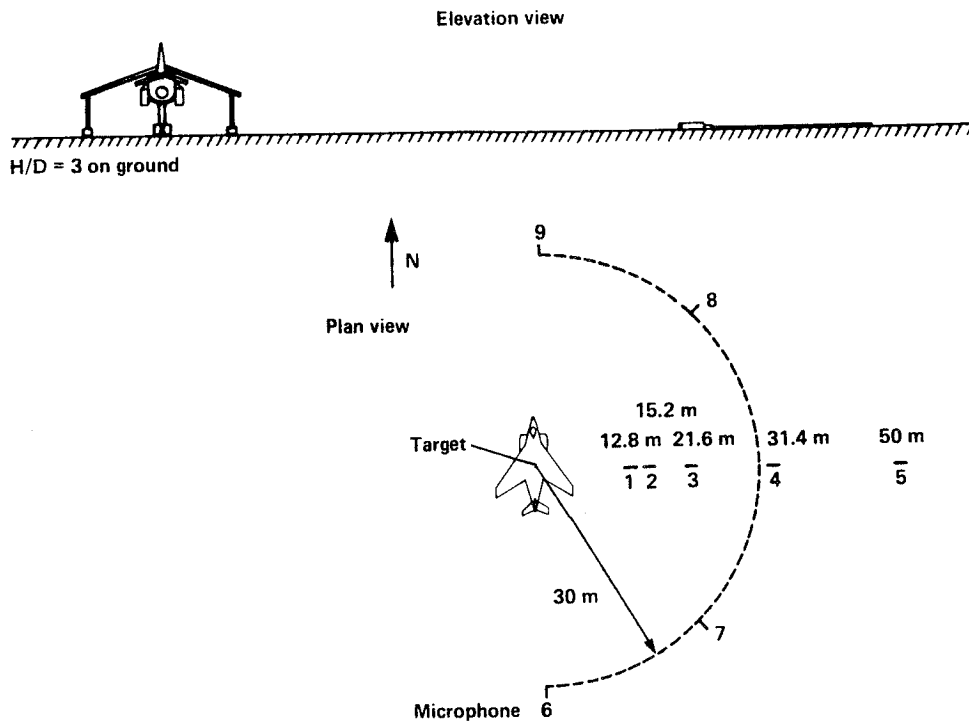


Figure 10 – Microphone layout at the landing site. The aircraft landed with the nozzle centroid over the target and the nose aimed north.

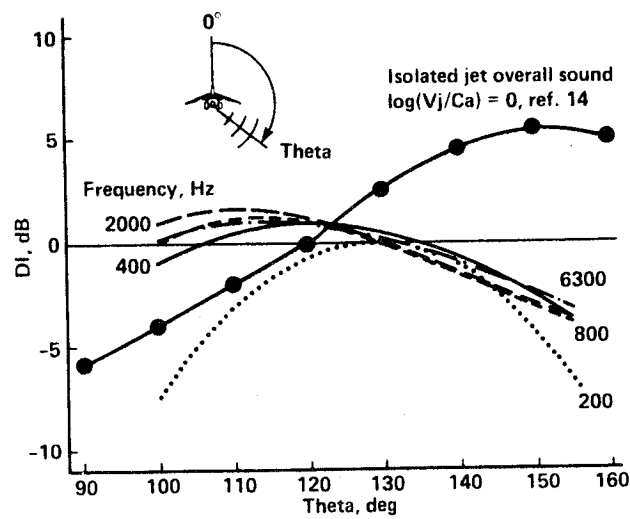


Figure 11 – Directivity of Harrier vertical jet noise during hover. DI is in vertical plane perpendicular to flight direction on the right side of the aircraft. Isolated jet directivity from Ref. 14 is included for comparison.

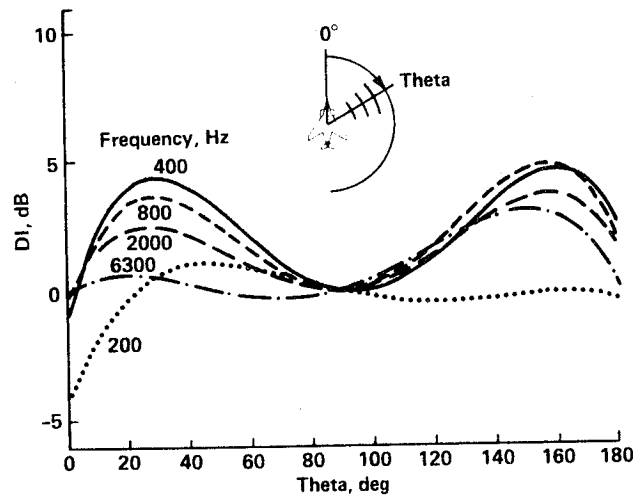
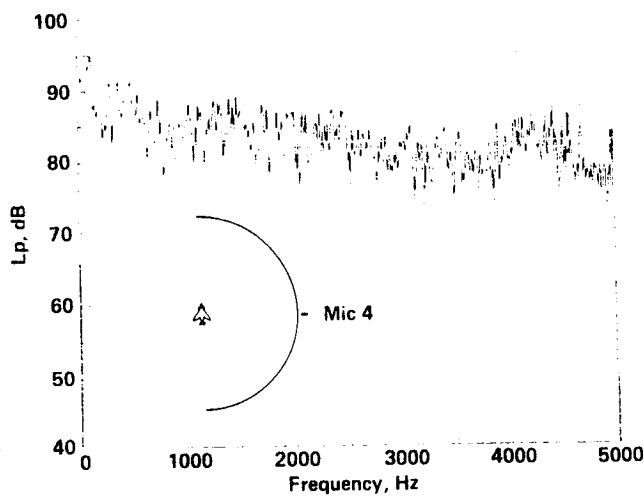
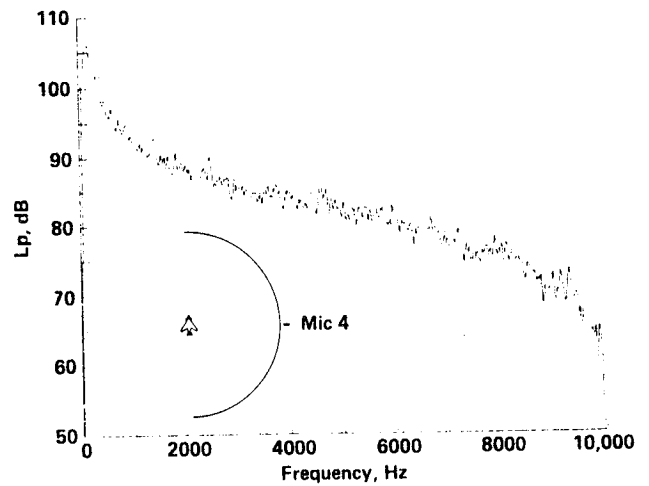


Figure 12 – Horizontal directivity of Harrier jet noise relative to 90° as measured by ground microphones on a semicircle to the right of the aircraft. The aircraft was hovering at 24.7 m altitude.

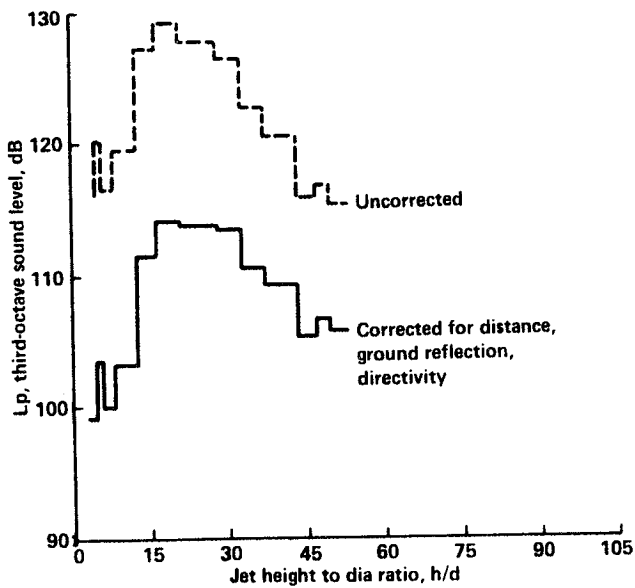


(a) Landing at $h/d = 4.4$, filter bandwidth = 12 Hz.

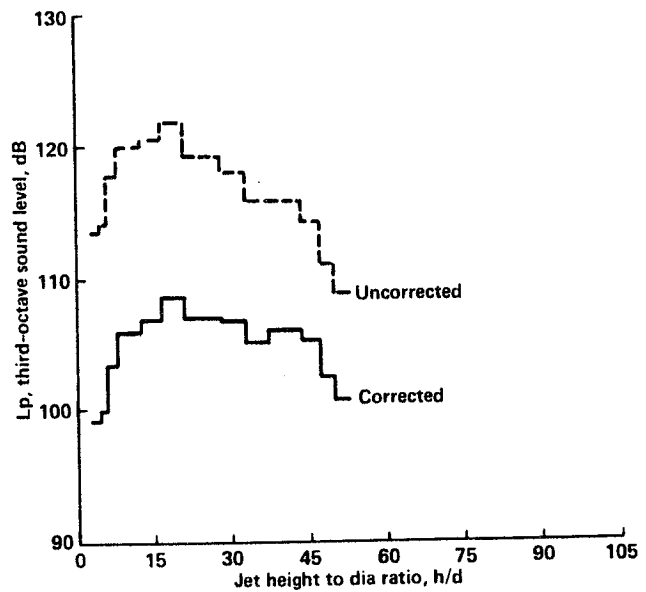


(b) Hover at 24.3 m ($h/d = 51$), filter bandwidth = 24 Hz.

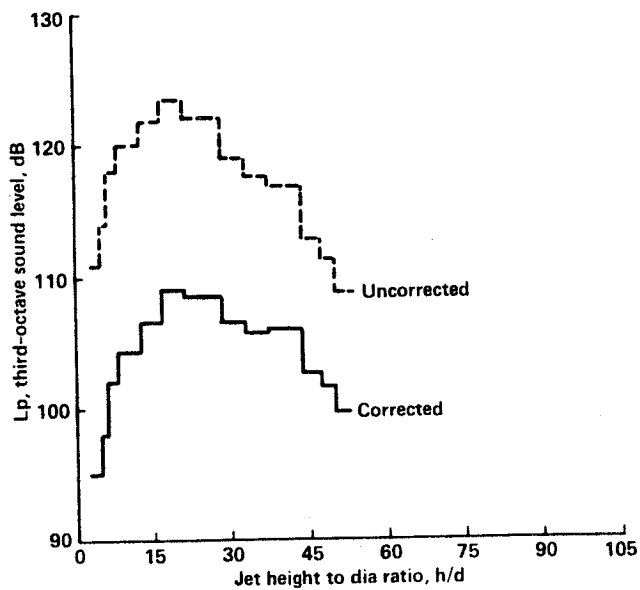
Figure 13 – Narrow-band spectra measured during landing and hover, microphone 4.



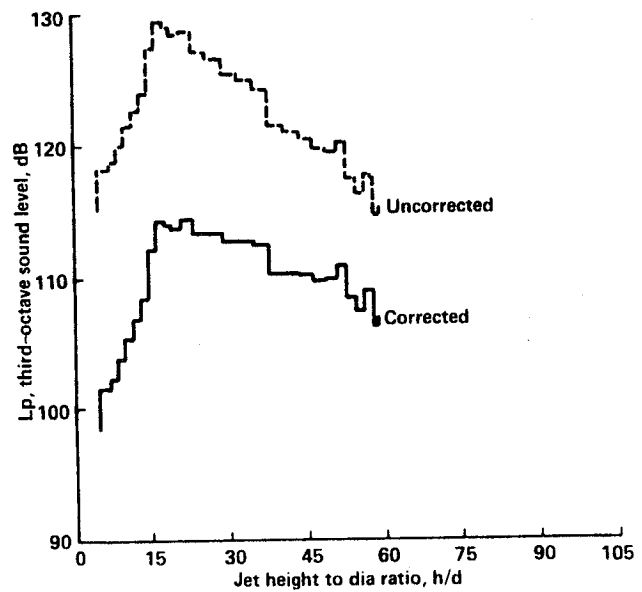
a) 200 Hz third-octave band, takeoff.



c) 4000 Hz third-octave band, takeoff.

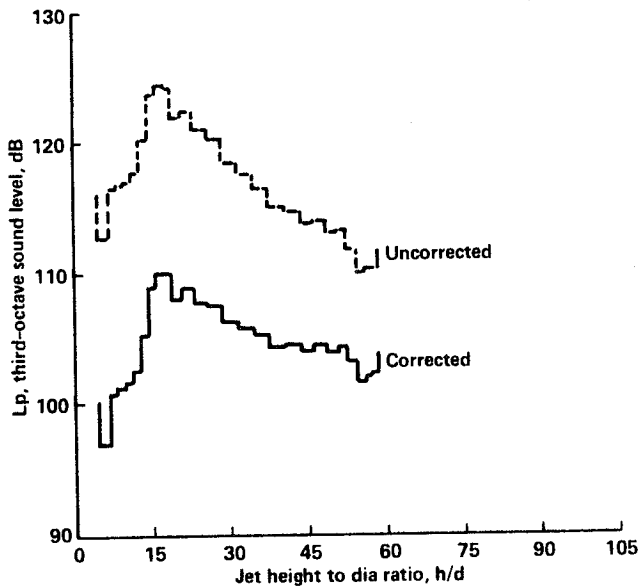


b) 1000 Hz third-octave band, takeoff.

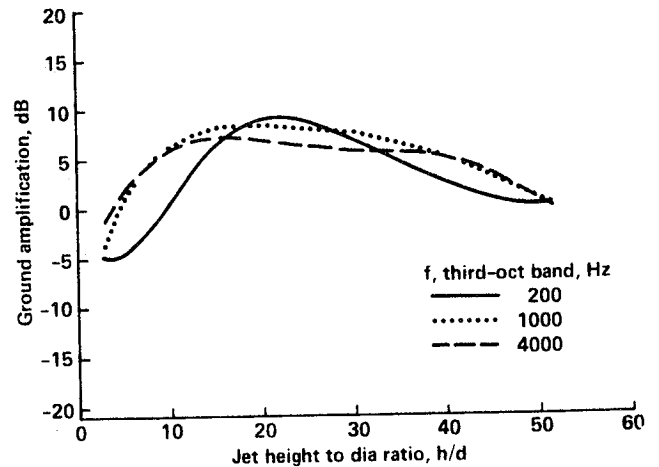


d) 200 Hz third-octave band, landing.

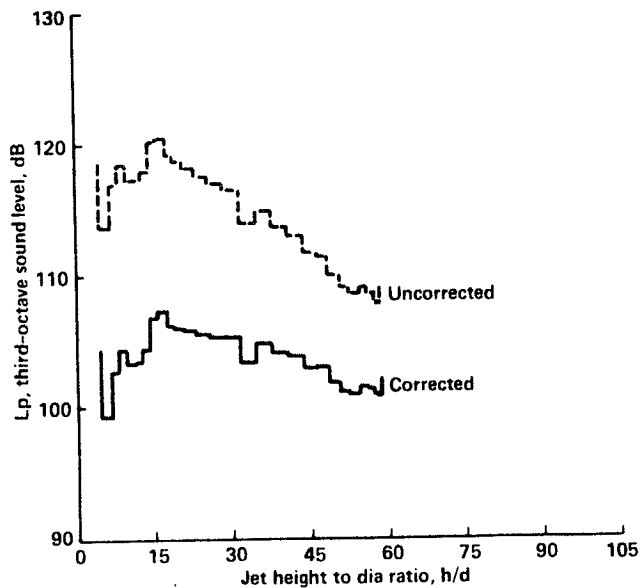
Figure 14 – Harrier third-octave noise levels measured 12.8 m from the landing site during vertical takeoff and landing (mic. 1); corrected and uncorrected noise levels.



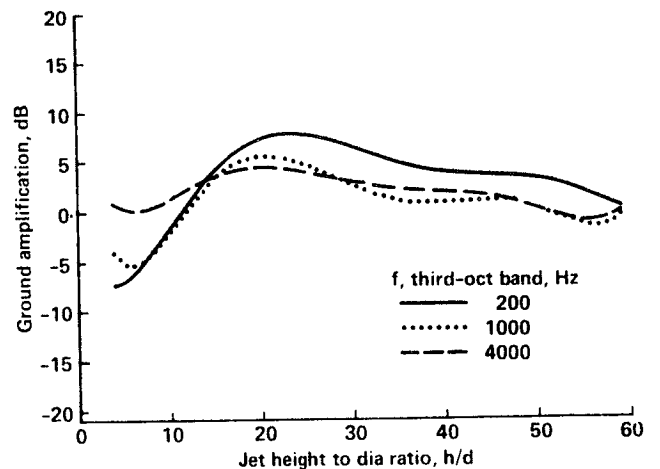
e) 1000 Hz third-octave band, landing.



a) 12.8 m from landing site, takeoff.



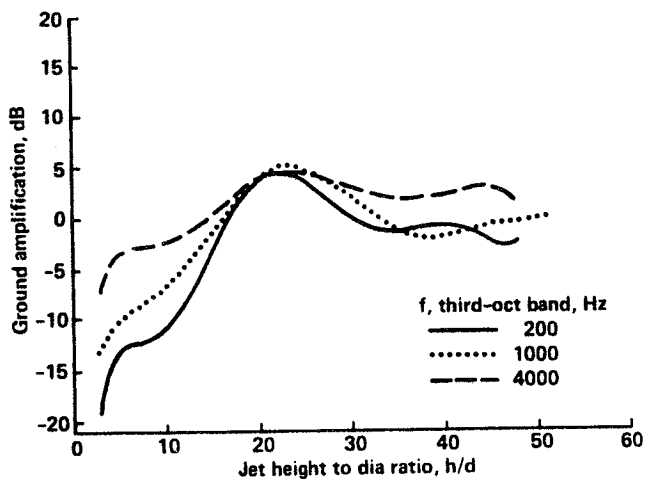
f) 4000 Hz third-octave band, landing.



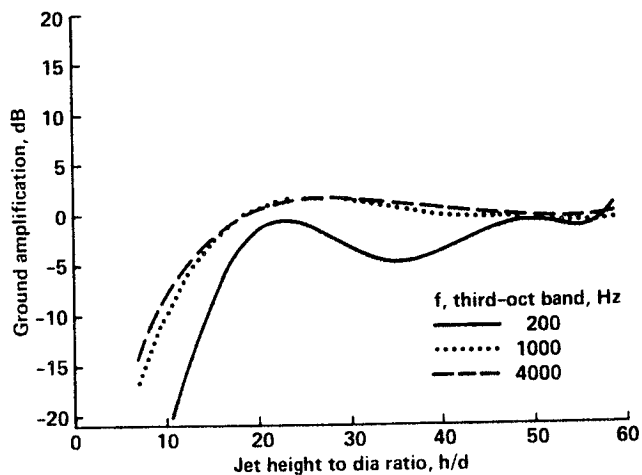
b) 12.8 m from landing site, landing.

Figure 14 – Concluded.

Figure 15 – Difference between corrected noise measured in and out of ground effect ($L_p(h/d \text{ max}) - L_p(h/d)$) at two distances from the landing target.



c) 50 m from landing site, takeoff.



d) 50 m from landing site, landing.

Figure 15 – Concluded.

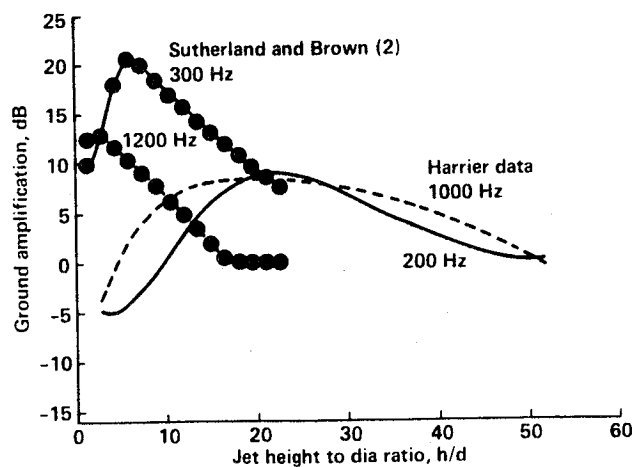
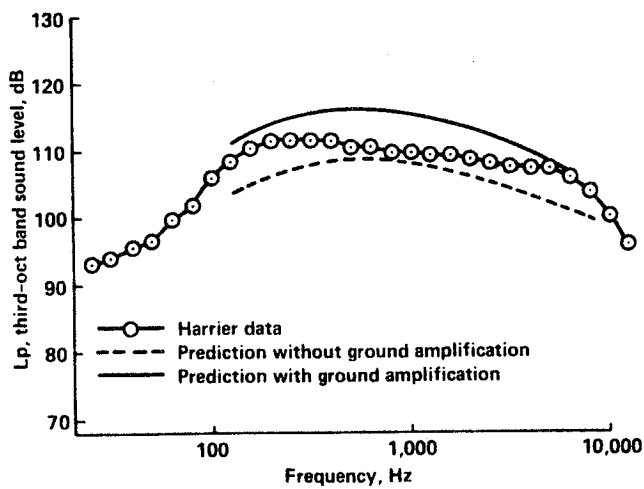
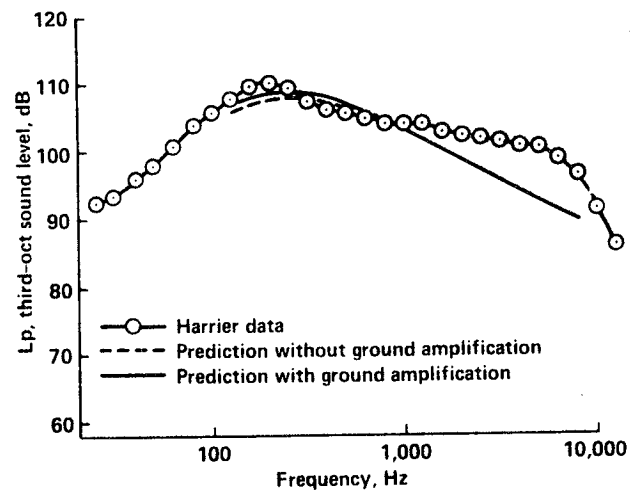


Figure 16 – A comparison of the data from Fig. 15(a) and the ground effect noise from Ref. 2.



a) $\theta = 111^\circ$, $h/d = 26$.



b) $\theta = 130^\circ$, $h/d = 58$.

Figure 17 – A comparison of Harrier hover noise and the complete prediction method including the directivity effects of Fig. 11. The hover data have been reduced by 6 dB to remove the pressure doubling at the ground microphone no. 4. The jet noise prediction was increased by 3 dB to simulate the two aft jets (forward jet noise was insignificant). $v_j = 447$ m/sec, $M_j = .93$, $T_j = 687^\circ$ K, pressure ratio = 1.72.



Report Documentation Page

1. Report No. NASA TM-102833		2. Government Accession No.		3. Recipient's Catalog No.	
4. Title and Subtitle The Prediction of STOVL Noise—Current Semi-Empirical Methods and Comparisons with Jet Noise Data				5. Report Date April 1990	
				6. Performing Organization Code	
7. Author(s) Paul T. Soderman				8. Performing Organization Report No. A-90187	
				10. Work Unit No. 505-61-11	
9. Performing Organization Name and Address Ames Research Center Moffett Field, CA 94035-1000				11. Contract or Grant No.	
				13. Type of Report and Period Covered Technical Memorandum	
12. Sponsoring Agency Name and Address National Aeronautics and Space Administration Washington, DC 20546-0001				14. Sponsoring Agency Code	
15. Supplementary Notes Point of Contact: Paul T. Soderman, Ames Research Center, MS 247-2, Moffett Field, CA 94035-1000 (415) 604-6675 or FTS 464-6675 Presented at 1990 SAE Aerospace Atlantic Conference, Dayton, Ohio, Apr. 23-26, 1990, and RAE International Powered Lift Conference, London, England, Aug. 29-31, 1990.					
16. Abstract <p>Current empirical models of several turbojet acoustic sources have been incorporated in a scheme for prediction of conventional or STOVL jet aircraft noise. The acoustic sources modeled were jet mixing noise, core noise, and broadband shock noise. The free-jet noise was then coupled with a new empirical equation for ground interaction noise generated by a vertically impinging jet. The modification of out-of-ground free-jet acoustic directivity pattern by a Harrier type nozzle installation was incorporated in the prediction of STOVL noise.</p> <p>The jet/ground interaction noise prediction is the result of a flight test of the NASA Ames Harrier jet aircraft that was operated in vertical takeoff and landing. Acoustic data measured with an array of ground level microphones showed ground amplification of jet noise that peaked at a jet height equal to 18 nozzle diameters. At jet heights below 18 nozzle diameters, far-field ground level noise decreased. It is suggested that the noise decrease was caused by refraction of sound upward by the jet ground sheet. Near-field noise on the airframe was not measured, but published near-field data are examined.</p> <p>Unlike numerous small-scale studies of jet impingement on a hard surface, in this study, no tones were found in the Harrier spectra. Implications for improved laboratory simulations of jet/ground interactions are discussed.</p> <p>The acoustic prediction method described here gives fairly good agreement with measured far-field noise of the Harrier aircraft during hover in and out of ground effect.</p>					
17. Key Words (Suggested by Author(s)) Aeroacoustics, STOVL, STOVL noise, Jet noise, Jet/ground interaction			18. Distribution Statement Unclassified-Unlimited Subject Category - 71		
19. Security Classif. (of this report) Unclassified		20. Security Classif. (of this page) Unclassified		21. No. of Pages 31	
				22. Price A02	